Application of Functional Amyloids in Morphological Control and in Self-assembled Composites

Elizabeth Carson Claunch

Thesis submitted to the faculty of the Virginia Polytechnic Institute and State University in partial fulfillment of the requirements for the degree of

Master of Science
In
Biological Systems Engineering

Justin R. Barone, Chair
Scott H. Renneckar
Ryan S. Senger

April 24, 2013
Blacksburg, VA

Keywords: amyloid; self-assembly; morphology; composite; Fourier transform infrared spectroscopy; atomic force microscopy; scanning electron microscope; 3 point bending

Application of Functional Amyloids in Morphological Control and in Self-assembled Composites

Elizabeth Carson Claunch

ABSTRACT

Amyloids are self-assembled protein materials containing β-sheets. While most studies focus on amyloids as the pathogen in neurodegenerative disease, there are instances of "functional" amyloids used to preserve life. Functional amyloids serve as an inspiration in materials design. In this study, it is shown that wheat gluten (WG) and gliadin:myoglobin (Gd:My) amyloid morphology can be varied from predominantly fibrillar at low polypeptide concentration to predominantly globular at high polypeptide concentration as measured at the nanometer scale using atomic force microscopy (AFM). The ability to control the morphology of a material allows control of its properties. Fourier transform infrared (FTIR) spectroscopy shows that at low concentration, fibrils require interdigitation of methyl groups on alanine (A), isoleucine (I), leucine (L), and valine (V). At higher concentration, globules do not have the same interdigitation of methyl groups but more random hydrophobic interactions. The concentration dependence of the morphology is shown as a kinetic effect where many polypeptides aggregate very quickly through hydrophobic interactions to produce globules while smaller populations of polypeptides aggregate slowly through well-defined hydrophobic interactions to form fibrils.

Functional amyloids also provide a means of creating a low energy process for composites. Poor fiber/matrix bonding and processing degradation have been observed in previous WG based composites. This study aims to improve upon these flaws by

implementing a self-assembly process to fabricate self-reinforced wheat gluten composites. These composites are processed in aqueous solution at neutral pH by allowing the fibers to form in a matrix of unassembled peptides. The fiber and the matrix are formed from the same solution, thus the two components create a compatible system with ideal interfacial interaction for a composite. The fibers in the composite are about 10 microns in diameter and can be several millimeters long. It has been observed that the number of fibers present along the fracture surface influences the modulus of the composite. In this study, self-assembled wheat gluten composites are formed and then characterized with 3-point bend (3PB) mechanical testing, scanning electron microscopy (SEM), and Fourier transform infrared (FTIR) spectroscopy.

ACKNOWLEDGEMENTS

I am extremely thankful for the abundance of support and encouragement that was given to me throughout my studies. I would like to thank my advisor, Dr. Justin Barone for his help and assistance throughout my graduate studies. You have given me great support and encouragement and I could not have accomplished all that I have without your guidance. I would also like to thank Dr. Scott Renneckar and Dr. Ryan Senger, your willingness to serve on my committee and your suggesting are greatly appreciated.

I also would like to thank Devin Ridgley for patiently teaching me all the lab techniques and procedures that I needed to complete this project. I would like to thank Caitlin Rippner for your daily support and optimism; you made this project more enjoyable.

Finally, I want to thank my family and friends for their continuous support and encouragement.

Table of Contents

Figures

Tables

Chapter 1 Introduction

Nature employs many complex techniques for designing materials. The challenge in science has been to understand the steps involved in these processes and then to take that knowledge and use it to design or improve synthetic systems that either attempt to mimic these techniques or to incorporate parts of them. One area of interest deals with proteins and the self-assembly process that they carry out in order to organize from the nano to the macro scale. Proteins are biological polymers and share many characteristics with synthetic polymers allowing for the use of similar characterization and processing techniques. These similarities provide proteins with many attributes as an alternative to the use of synthetic polymers.

1.1 Protein structural properties

Rarely do synthetic materials exhibit a combination of desirable features. They are typically either strong with little elasticity (ceramics, glass, silicon) or weak with high elasticity (rubber).[1, 2] Typically only expensive, exotic materials such as Kevlar and carbon fibers are manufactured with unique combinations of properties, such as high strength and low density. Relating two properties of a material was pioneered by Ashby and resulted in diagrams similar to those found in figure 1.1 which shows Young's Modulus (E) as a function of density (ρ) and fracture toughness (K_{1c}) as a function of Youngs Modulus.[3] These diagrams are useful for comparing ratios of two properties, and from them a material of maximum performance can be selected. For graph 1.1 a, the most ideal region to be in is a combination of high E and low ρ and for graph 1.1 b both high E and toughness are desirable. Most of the expensive, exotic materials, as

mentioned, reside in these areas. The positions of protein fibers have been added to the diagrams to show that they also reside in this unique position and can be competitive with those materials. Proteins are capable of combining high strength and toughness. Spider silk is known to have a tensile strength on the level of steel or Kevlar and is also extremely elastic.[2, 4, 5] The properties of spider silk become even more impressive when normalized by its density.[2, 4] These unique properties of proteins, however, exist for very different reasons than materials that they share the regions with. It is known that a protein's material properties are affected by the molecular structure and it is suggested that the occurrence of properties is due to hierarchical features of protein materials.[1, 2]

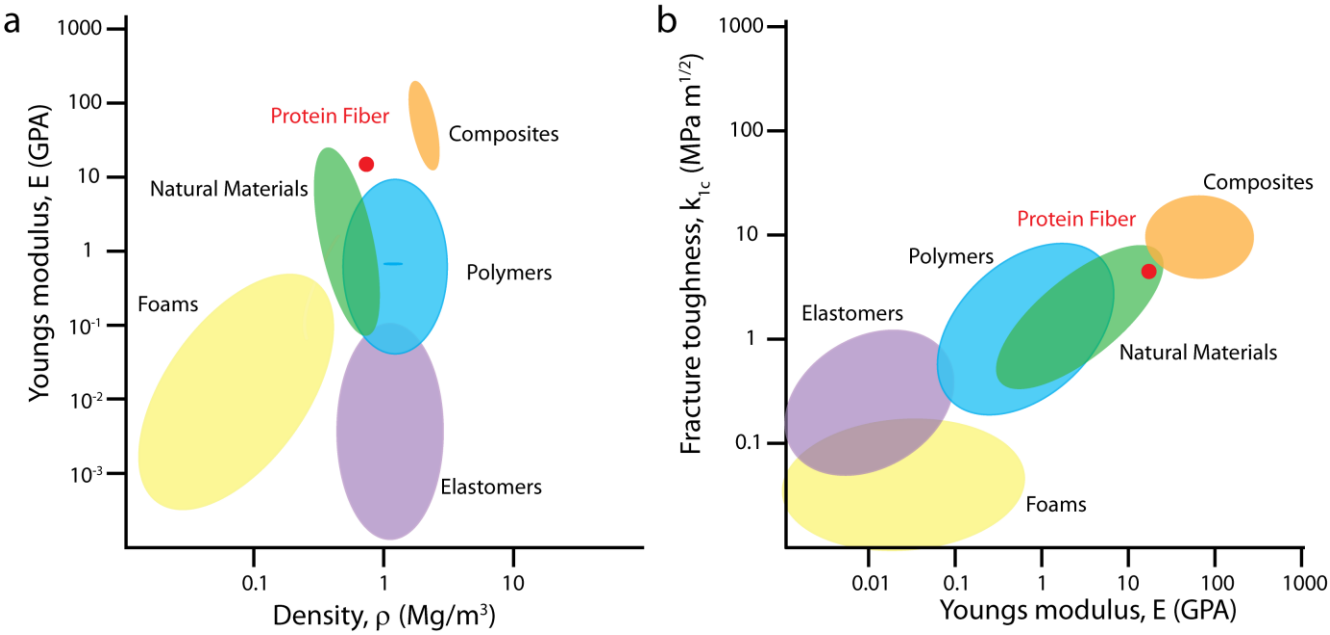

Figure 1.1 Ashby plots for (a) Young's modulus as a function of density and (b) fracture toughness as a function of Young's modulus show that protein fibers reside in unusual regions typically occupied by expensive, exotic materials. Protein fibers have a very unusual combination of high rigidity and toughness.

Proteins are the main structure component of a variety of materials such as cells, spider silk, bone, keratin, collagen, and elastin.[4, 6, 7] They are biopolymers that contain up

to 20 different types of amino acids, which can be thought of as monomers.[7] These monomers contribute to the structure of the protein. Cysteine is an amino acid that has been shown to stabilize hydrophobic interactions and contribute to the more organized domain of the protein. In Keratin, oxidation of cysteine thiol groups results in disulphide bonds that can cross-link both intermolecularly and intramolecularly.[6] Like with cross-linking of the crystalline regions of a polymer the stability and stiffness of keratin increases with the number of crosslinks.

1.1.1 Secondary structure

The spatial arrangement of amino acids in peptide chains makes up the secondary structure of the protein.[6] Secondary structure is important in determining the function and properties of the protein, therefore spectroscopy techniques are often used to characterize the type and amount of each secondary structure component.[2, 6, 8] The peptide group is the most characteristic functional group within a protein. The vibrations of the atoms in this group give rise to different vibrational features. Emphasis is often placed on Amide I, which is a result of C=O stretching of the peptide backbone, and appears between 1680 and 1600 cm^{-1} on the spectra.[9, 10] This group is conformationally sensitive, and its position is characteristic of several secondary structures, including cross-β, α-helix, β-sheet and random coil.[6, 9, 10]

Different secondary structures have different properties much like different regions a polymer domain. Some regions of a protein consist of β-sheets which are highly organized crystalline structures, while other regions know as random coil are amorphous regions with no organization. Different secondary structures have different mechanical properties and the organization of these domains play into the overall material properties. Through a comparative study, Buehler and Keten suggested that α-helix protein domains

provide elasticity at large deformation while the β-sheet domains provides strength under shear loading.[2] Spider silk has a large β-sheet content which is why it is strong. Spiders are also able to generate different fibers for different uses, with each fiber having its own secondary structure composition.[9]

1.1.2 Protein folding

Another aspect of proteins that contributes to their structural properties is how they fold. Protein folding describes the process that occurs when a protein structure assumes its functional shape or conformation, also known as the native structure. This area of study is largely uncharted territory, due to the complexity of the process. Much can be learned from the way that proteins fold, but understanding what happens when proteins don't fold as expected is also extremely fascinating and beneficial. When a protein fails to fold into its native structure, inactive proteins are produced. A popular area of interest associated with protein misfolding are amyloid fibers which are a complex natural system that uses proteins for self-assembly.[11]

1.2 Protein self-assembly

Self-assembly is any system that spontaneously overcomes the free energy needed to go from a lower to higher level of structural complexity. Electrostatic interactions, hydrogen bonding, hydrophobic interactions, and shape can all play roles in the self-assembly process which is driven by an overall reduction in free energy of the system at defined process conditions.[11] Unlike extrusion, another process nature uses to make protein fibers such as spider silk and β-keratin that aligns the β-sheet along the axis, self-assembly allows the β-sheet to align perpendicular to the fiber axis.[12-14] This secondary structure is termed cross-β and results in a robust material. Amyloids are self-assembled protein materials containing β-sheets.[15-19] This amyloid form is thought of as an

alternative form of protein structure that is different than a proteins native structure, but is just as organized because of the cross beta sheets.[20]

1.2.1 Amyloids

The presence of cross-β sheets along with fibrillar structure, and bio-refringence pattern are all used to determine if a fiber is amyloid. Fibrillar structure is determined by microscopy methods such as AFM or SEM. According to Knowles et. al. they typically appear as an unbranched filament that are usually a few nanometers in diameter and up to a micrometer in length.[21] The presence of cross-beta sheets is determined with spectroscopy methods such as Fourier transform infrared spectroscopy, Raman spectroscopy, nuclear magnetic resonance, and x-ray diffraction.[2] Biorefringence is a pattern observed with binding dyes such as congo red. Many unique features result from the self-assembly process in which amyloids are formed.

Amyloids or prions are the fibrils that and are associated with neurodegenerative diseases such as such as Alzheimer's, Parkinson's, and Huntington's Diseases.[15, 17, 18, 22] These occur from a deposition of fibrillar aggregates either within or around neurons in specific brain regions. Alzheimer's for example is thought to occur when normally soluble proteins are deposited into an accumulation of amyloid fiber aggregates.[20, 23] Neurodegenerative diseases are most often associated with old age, when the functional capacity of a molecular chaperone and other aspects of protein quality control decrease, resulting in an increased tendency for proteins to become misfolded or damaged during aging.[23, 24] Amyloids have extremely good thermodynamic and mechanical stability.[19, 25] A testimony to this is that there is no known cure for these diseases.

1.2.2 Functional amyloids

Functional amyloids are those that are not associated with destruction or disease but rather occur in nature as a mechanism for survival and preservation.[17, 20, 26] Examples include barnacle cement [27-30], fungal spore coatings[26, 31], bacterial hyphae [32-34], and insect silk.[13, 35, 36] There are many unique features and characteristics associated with these structures. Similar to spider's that can change the secondary structure of their silk for different functions, a barnacle can alter the amyloid content of its adhesive. This allows the barnacle to change the morphology of its adhesive and adhere to virtually any surface.[27, 30, 37] Like the barnacle which is one of nature's strongest adhesives, materials that contain amyloids exhibit exceptional properties. Good mechanical properties such as high stiffness, elasticity, and resistance[19, 25] can exist because amyloids are a structure different from the typical folded structure and features that would normally be buried in the native state, such as hydrophobic surfaces and regions of unstructured polypeptide backbone are usually exposed.[24, 38] Amyloids are also typically energetically favorable compared with their soluble native state and are highly stable structures.[20]

The outstanding physical properties and observed functional role of amyloids in nature make them an excellent model for biomimicry.[39] Self-assembly is a bottom up approach that holds great promise for the development of submicron scale materials.[2, 11, 19, 25] This type of processing can be used to create multifunctional materials by self-assembly of structures over many length and timescales.[40] Amyloid fibrils are also independent of amino acid sequence and can be formed by a wide range of proteins under denaturing conditions.[20, 21, 41] This makes them adaptable to many applications.

Morphology and structure play into how a protein will function. Proteins have many unique features that make them a desirable asset to the materials industry. Along

with this, they also have the added benefit of being more environmentally friendly than most synthetic, petroleum based polymers.

1.3 Outline of thesis

The following chapters will outline two amyloid forming, protein systems. It has been determined that structure plays a role in the overall protein structure and that amyloids are an inspiration for design of materials. The next chapter examines the role that concentration plays in determining the morphology and thus the properties of amyloid forming WG and gliadin:myoglobin (Gd:My) systems. Amyloid morphology can be varied from predominantly fibrillar at low polypeptide concentration to predominantly globular at high polypeptide concentration. The concentration dependence of the morphology is shown as a kinetic effect where many polypeptides aggregate very quickly through hydrophobic interactions to produce globules while smaller populations of polypeptides aggregate slowly through well-defined hydrophobic interactions to form fibrils. The third chapter takes more of a material design approach and examines the role that amyloids can fulfill as the structural component for a composite. Self- assembly can be used to form a composite composed entirely of WG. These composites are formed from solution in which two peptides form the fiber and the remaining peptides stay unassembled to form the matrix. The self-assembly process avoids processing degradation that can be associated with heat and pressure, typically used in protein processing. Another added benefit is that the composite is formed from peptides in the same solution so there is great interfacial interaction between the fiber and the matrix. Chapter four concludes the thesis with a summary of the research presented and suggestions for future work and application of the amyloid forming systems.

References

1. Buehler, M. J.; Yung, Y. C., How protein materials balance strength, robustness, and adaptability. *HFSP journal* **2010,** 4, (1), 26-40.

2. Buehler, M.; Keten, S., Elasticity, strength and resilience: A comparative study on mechanical signatures of α-Helix, β-sheet and tropocollagen domains. *Nano Res.* **2008,** 1, (1), 63-71.

3. Hull, D.; Clyne, T. W., *An introduction to composite materials*. 2nd ed.; Cambridge University Press: Cambridge ; New York, 1996; p xvi, 326 p.

4. Tarakanova, A.; Buehler, M., A Materiomics Approach to Spider Silk: Protein Molecules to Webs. *JOM* **2012,** 64, (2), 214-225.

5. Becker, N.; Oroudjev, E.; Mutz, S.; Cleveland, J. P.; Hansma, P. K.; Hayashi, C. Y.; Makarov, D. E.; Hansma, H. G., Molecular nanosprings in spider capture-silk threads. *Nat Mater* **2003,** 2, (4), 278-283.

6. Gremlich, H.-U.; Yan, B., *Infrared and raman spectroscopy of biological materials*. M. Dekker: New York, 2001; p ix, 581 p.

7. Fried, J. R., *Polymer science and technology*. 2nd ed.; Prentice Hall Professional Technical Reference: Upper Saddle River, NJ, 2003; p xvii, 582 p.

8. Pelton, J. T.; McLean, L. R., Spectroscopic Methods for Analysis of Protein Secondary Structure. *Analytical Biochemistry* **2000,** 277, (2), 167-176.

9. Salzer, R.; Siesler, H. W., *Infrared and Raman spectroscopic imaging*. Wiley-VCH: Weinheim, 2009; p xx, 510 p.

10. Schrader, B.; Bougeard, D., *Infrared and Raman spectroscopy : methods and applications*. VCH: Weinheim ; New York, 1995; p xx, 787 p.

11. McGrath, K.; Kaplan, D., *Protein-based materials*. Birkhäuser: Boston, 1997; p xx, 429 p.

12. Fraser, R. D. B.; MacRae, T. P., *Conformation in Fibrous Proteins and Related Synthetic Polypeptides*. Academic Press: New York, 1973.

13. Parker, K. D.; Rudall, K. M., Structure of the silk of *Chrysopa* egg-stalks. *Nature* **1957,** 179, 905-906.

14. Jin, H.-J.; Kaplan, D. L., Mechanism of silk processing in insects and spiders. *Nature* **2003,** 424, 1057-1061.

15. Dobson, C. M., Protein misfolding, evolution and disease. *Trends in Biochemical Science* **1999,** 24, 329-332.

16. Dobson, C. M., Sali,A. and Darplus,M., Protein folding: a perspective from theory and experiment. *Angew. Chem (Int. Ed.)* **1998,** 37.

17. Chiti, F.; Dobson, C. M., Protein misfolding, functional amyloid, and human disease. *Annual review of biochemistry* **2006,** 75, 333-66.

18. Dobson, C. M., Protein folding and misfolding. *Nature* **2003,** 426, 884-890.

19. Paparcone, R.; Buehler, M. J., Failure of Alzheimer's Aβ (1–40) amyloid nanofibrils under compressive loading. *JOM* **2010,** 62, (4), 64-68.

20. Knowles, T. P. J.; Buehler, M. J., Nanomechanics of functional and pathological amyloid materials. *Nat Nano* **2011,** 6, (8), 469-479.

21. Knowles, T. P.; Fitzpatrick, A. W.; Meehan, S.; Mott, H. R.; Vendruscolo, M.; Dobson, C. M.; Welland, M. E., Role of Intermolecular Forces in Defining Material Properties of Protein Nanofibrils. *Science* **2007,** 318, (5858), 1900-1903.

22. Prusiner, S. B., Prions. *Proceedings of the National Academy of Sciences* **1998,** 95, (23), 13363-13383.

23. Dobson, C. M., Protein folding and misfolding. *Nature* **2003,** 426, (6968), 884-890.

24. Hartl, F. U.; Hayer-Hartl, M., Converging concepts of protein folding in vitro and in vivo. *Nat Struct Mol Biol* **2009,** 16, (6), 574-581.

25. Paparcone, R.; Cranford, S.; Buehler, M. J., Compressive deformation of ultralong amyloid fibrils. *Acta Mechanica Sinica* **2010,** 26, (6), 977-986.

26. Fowler, D. M.; Koulov, A. V.; Balch, W. E.; Kelly, J. W., Functional amyloid-From bacteria to humans. *TRENDS in Biochemical Sciences* **2007,** 32, (5), 217-224.

27. Barlow, D. E.; Dickinson, G. H.; Orihuela, B.; Kulp, J. L.; Rittschof, D.; Wahl, K. J., Characterization of the Adhesive Plaque of the Barnacle Balanus amphitrite: Amyloid-Like Nanofibrils Are a Major Component. *Langmuir* **2010,** 26, (9), 6549-6556.

28. Kamino, K.; Odo, S.; Maruyama, T., Cement Proteins of the Acorn-Barnacle, Megabalanus rosa. *The Biological Bulletin* **1996,** 190, (3), 403-409.

29. Kamino, K.; Inoue, K.; Maruyama, T.; Takamatsu, N.; Harayama, S.; Shizuri, Y., Barnacle Cement Proteins. *Journal of Biological Chemistry* **2000,** 275, (35), 27360-27365.

30. Sullan, R. M. A.; Gunari, N.; Tanur, A. E.; Chan, Y.; Dickinson, G. H.; Orihuela, B.; Rittschof, D.; Walker, G. C., Nanoscale structures and mechanics of barnacle cement. *Biofouling* **2009,** 25, (3), 263-275.

31. Gebbink, M. F. B. G.; Claessen, D.; Bouma, B.; Dijkhuizen, L.; Wosten, H. A. B., Amyloids-A functional coat for microorganisms. *Nature Reviews Microbiology* **2005,** 3, 333-341.

32. Ben Nasr, A.; Olsen, A.; Sjobring, U.; Muller-Esterl, W.; Bjorck, L., Assembly of human contact phase proteins and release of bradykinin at the surface of curli-expressing *Escheria coli*. *Molecular Microbiology* **1996,** 20, (5), 927-935.

33. Hammer, N. D.; Schmidt, J. C.; Chapman, M. R., The curli nucleator protein, CsgB, contains an amyloidogenic domain that directs CsgA polymerization. *Proceedings of the National Academy of Sciences* **2007,** 104, (30), 12494-12499.

34. Wang, X.; Chapman, M. R., Curli provide the template for understanding controlled amyloid propagation. *Prion* **2008,** 2, (2), 57-60.

35. Parker, K. D.; Rudall, K. M., The silk of the egg-stalk of the green lace-wing fly. *Nature* **1957,** 179, 905-906.

36. Weisman, S.; Trueman, H. E.; Mudie, S. T.; Church, J. S.; Sutherland, T. D.; Haritos, V. S., An unlikely silk: The composite material of green lacewing cocoons. *Biomacromolecules* **2008,** 9, (11), 3065-3069.

37. Wiegemann, M.; Watermann, B., Peculiarities of barnacle adhesive cured on non-stick surfaces. *Journal of Adhesion Science and Technology* **2003,** 17, (14), 1957-1977.

38. Horwich, A. L.; Fenton, W. A.; Chapman, E.; Farr, G. W., Two families of chaperonin: physiology and mechanism. *Annual review of cell and developmental biology* **2007,** 23, 115-45.

39. Knowles, T. P. J.; Oppenheim, T. W.; Buell, A. K.; Chirgadze, D. Y.; Welland, M. E., Nanostructured films from hierarchical self-assembly of amyloidogenic proteins. *Nat Nano* **2010,** 5, (3), 204-207.

40. Buehler, M. J.; Cranford, M. J., Materiomics: biological protein materials, from nano to macro. **2010**.

41. Knowles, T. P.; Oppenheim, T. W.; Buell, A. K.; Chirgadze, D. Y.; Welland, M. E., Nanostructured films from hierarchical self-assembly of amyloidogenic proteins. *Nature nanotechnology* **2010,** 5, (3), 204-207.

Chapter 2 Changing morphology of self-assembled polypeptide structures

2.1 Introduction

2.1.1 Amyloid fibers

Amyloids are self-assembled protein materials containing β-sheets.[1-4] The most common context for amyloids is in pathogenic protein misfolding or "prion" diseases such as Alzheimer's, Parkinson's, and Huntington's Diseases.[1, 3-5] Self-assembly begins when a protein molecule "misfolds", straightens out, and hydrogen bonds to another misfolded, straight protein molecule to build the β-sheet. In disease progression, the field is focused on small, isotropic β-sheet aggregates or "oligomers" as the pathogen and how to stop their formation. These small β-sheet aggregates can continue to aggregate into protofibrils with diameters of ~10^0-10^1 nm and lengths of >10^2 nm.[6-38] Several protofibrils can then aggregate together into the prion "plaques" that have been studied extensively and are the hallmark of advanced prion disease. In these nanometer amyloid fibrils, the protein chain axis is perpendicular to the fibril axis and thus the β-sheets are termed "cross-β" sheets.[39] In contrast, the protein chain axis and resulting β-sheets in natural silk and β-keratin fibers are aligned with the fiber axis. This results from the applied deformation required to form the silk or β-keratin fiber, i.e., pultrusion or extrusion, respectively.[39-41]

There is a smaller class of amyloid that performs beneficial functions in nature. These are termed "functional" amyloids and occur in nature as a mechanism for survival and preservation.[3, 42, 43] Barnacle cement has been shown to be a rigid, strong, and tough adhesive and uses alternating hydrophobic and hydrophilic amino acid regions to form an insoluble cross-β fibril, which contributes to the adhesive's properties.[44-47] The

bacterium *Streptomyces coelicolor* and fungus *Neurospora crassa* use amyloids to form protective coatings and hyphae.[43, 48] *Escherichia coli* will secrete curli proteins CsgA and CsgB to form fibrous amyloid hyphae on the cell surface.[49-51] Insects of the *Chrysopidae* family form amyloid silks to protect their eggs.[39, 52, 53] Amyloid fibrils have been shown to have moduli comparable to spider silk, specific moduli comparable to steel, and can be formed without electrospinning.[42, 54-58] Amyloid fibrils have also shown great solvent and temperature resistance and the fact that no known cure exists for prion disease is a testament to the robustness of the self-assembled β-sheet structure.[59] The outstanding physical properties and observed functional role of amyloids in nature make them an excellent model for biomimicry.[60]

2.1.2 Changing morphology of barnacle cement

In particular, the barnacle cement example is interesting. Barnacle cement has the ability to withstand large hydrodynamic forces through an optimized combination of rigidity, strength, and toughness.[44, 47, 61] Barnacle cement is composed of 90% protein.[45, 46, 62] Unlike mussel adhesive, the barnacle adhesive does not rely on covalent cross-linking between DOPA molecules on adjacent proteins for high properties.[63-65] Rather, barnacle cement relies on self-assembled amyloid protein fibrils to reinforce the cement akin to a fiber composite.[44, 46, 47] Barnacle cement shows a morphology that is both globular and fibrillar and the ratio of each structure can be varied depending on the physical properties of the surface to which it is adhered. Wiegemann and Watermann found that barnacle cement grown on low energy polydimethyl siloxane (PDMS) surfaces produced a loosely bound (low density) fibrous mat morphology.[66] However, barnacle cement grown on high energy aluminum foil produced a dense globule morphology.

Berglin and Gatenholm showed that barnacle cement grown on low energy, low modulus PDMS produced a globular morphology that was thick and rubbery and did not contain calcium.[67] Barnacle cement grown on medium energy, high modulus polymethyl methacrylate (PMMA) produced a more continuous film formed from fused globules that contained calcium that they postulated aided the globule fusion. Sullan et. al. grew barnacles on PDMS and then transferred them to glass coverslips for 2 days for atomic force microscopy (AFM) measurements.[47] The barnacle cement had a mixed morphology of mostly nanometer-sized fibrils in a mat morphology with some globules and large, rod aggregates about 0.5 μm in diameter. The fibrils and rods were found to be amyloids. Transferring the barnacles to aluminum foil for a week prior to scanning electron microscopy (SEM) and energy dispersive x-ray (EDX) analysis displayed a morphology with more large rods. Sullan et. al. showed with force spectroscopy and AFM indentation that the rods were more rigid than the globules and that the cement displayed a "sawtooth" force-extension pattern on 1-100 nm scale, which is indicative of tough materials. Barlow et. al. found barnacle cement to contain a much higher amyloid content than Sullan et. al.[44] Barlow et. al. grew barnacles on quartz and PDMS coated glass. On PDMS, the barnacle cement had a globular morphology at the center of the baseplate with a dense fibril mat forming along the radius of the baseplate. On quartz, there were sparse fibrils in the center with more dense fibrils along the radius. Early fibrils were 2-5 nm and fully formed fibrils were 25 nm in diameter. The fibrils had a periodicity that was probably the chiral "twist" well-known in amyloids.[29, 35-38] Thus, barnacles can shift their morphology from fibrous to globular with mixtures of the two possible and the fibrils can range in size. The shifting morphology highly depends on the

surface the cement was grown on and the environmental conditions and the discrepancies in the various studies are probably a result of this. For instance, the study of Barlow et. al. shows that the morphology varies along the radius of the baseplate so where you look at the cement is important. In addition, transferring the barnacle between high and low energy substrates may produce new, secondary cement of different morphology.

These studies show that the barnacle has the distinctive ability to attach to virtually any surface. The organism must have a simple method for manipulating protein synthesis and/or secretion to affect morphology. The ability to attach to any surface means that the protein adhesive can shift its equilibrium structure and resulting morphology. Tryptic hydrolysates of wheat gluten (WG) and tryptic hydrolysates of gliadin mixed with unhydrolyzed myoglobin (Gd:My) can be used to self-assemble cross-β fibrils similar to the fibrous amyloid structures of barnacle cement.[55, 68-70] In this study, WG and Gd:My are used as model systems to study the morphology of self-assembled polypeptide structures a function of polypeptide concentration in aqueous solution and the number of layers of polypeptide solution of a single concentration deposited on a high energy surface. Polypeptide secondary structure formation is assessed with Fourier transform-infrared (FT-IR) spectroscopy and the morphology of solutions dried on mica is characterized with atomic force microscopy (AFM).

2.2 Materials and Methods

2.2.1 Protein solutions.

Several concentrations (15, 25, 35, 45 and 55 mg/ml) of wheat gluten (WG) (MP Biomedicals, LLC, Solon, OH) was hydrolyzed with trypsin (Type I from bovine pancreas, Sigma-Aldrich, St. Louis, MO) at a constant 1:67 w/w enzyme to substrate

ratio in 80 ml of de-ionized water at pH 8 and 37°C. Gliadin (Gd, TCI America, Portland, OR, UniProt P04721) was dissolved in 800 ml of pure water at a concentration of 25 mg/ml. Trypsin was added at the same ratio and the solution was maintained at pH 8 and 37^{o}C for three days to ensure that hydrolysis was complete. The times have been confirmed as being after complete hydrolysis but before aggregation.[55, 68, 69] Gd was poured into Teflon-coated aluminum foil trays and allowed to dry at ambient conditions under a fume hood. The dried, hydrolyzed Gd was combined with myoglobin (My, from equine skeletal muscle, Sigma-Aldrich, St. Louis, MO, UniProt P68082) in 80 ml of DI water at a molar ratio of 0.36:0.64 (Gd:My) and concentrations of 15, 25, 35, 45 and 55 mg/ml. These were maintained at pH 8 and 37°C for 20 days.

2.2.2 Fourier transform infrared (FTIR) spectroscopy.

Attenuated total reflectance (ATR) FTIR spectra of the incubating solutions were recorded daily on a Thermo Nicolet 6700 FTIR Spectrometer (Thermo Fisher Scientific Inc., Waltham, MA) with a 45^{o} ZnSe crystal trough. The spectra were collected using 256 scans at 4 cm^{-1} resolution from 4000-525 cm^{-1}. The spectrum of the solvent without polypeptide was used as a background and then subtracted from the solution spectrum to reveal the polypeptide absorbances. After twenty days the solutions were dried on Teflon coated aluminum foil at ambient conditions under a fume hood. FTIR spectra of dried solutions were taken with a Smart Orbit ATR Diamond Crystal (Thermo Fisher Scientific Inc., Madison, WI). The spectra were collected using 256 scans at 4 cm^{-1} resolution from 4000-525 cm^{-1} with a blank background.

2.2.3 FTIR amide I analysis.

The Amide I absorbance originates in the peptide bond carbonyl stretch, ν(C=O), and can be correlated to protein secondary structure.[71] Most polypeptides and proteins are not purely of one secondary structure and thus the Amide I absorbance is formed through contributions from all of the secondary structures present. It is possible to "deconvolute" the Amide I absorbance into its secondary structure components by representing it as a sum of peaks assigned to each structure.[53, 72-75] The area of each peak is representative of the molar concentration of that particular secondary structure. The spectral region from 1720−1580 cm^{-1} was isolated and manually smoothed with the Savitzky-Golay algorithm using 9-13 points. Next, the second derivative of the Amide I spectral region was taken without filtering to identify the individual Amide I components. Fourier self-deconvolution (FSD) was performed with Happ-Genzel apodization by setting enhancement to 2-3 and adjusting the bandwidth until absorbance maxima matched the second derivative minima.[44, 76, 77] Using the "Peak Resolve" feature of OMNIC v8.1, the Amide I absorbance was fit to a series of Gaussian/Lorentzian peaks matching the FSD. The Peak Resolve feature used the Fletcher-Powell-McCormick algorithm to fit the peaks.[78] Amide I fitting was performed with a constant baseline, a target noise of 10.0, and an initial full width at half-height (FWHH) of 3.857. The goodness of fit, in the form of an F value, was less than 0.5%.

2.2.4 Atomic force microscopy (AFM).

Two types of studies were conducted, one involving layering of one concentration of solution and the other involving five concentrations of solution. At 0, 4, 8, 12, 16, and 20 days, 50 μl of the solution was spin coated on freshly cleaved mica at 4000 rpm for 1

minute. For the layering study, 50 µl of the 25 mg/ml WG solution was spin coated 3, 5, and 10 times to create layers of WG on the mica. The varying concentrations of WG and of Gd:My were spin coated at one 50 µl layer each. Spin coating dries the sample quickly and does not allow further aggregation, thus it serves as a "snapshot" of aggregation at a particular time. Images of aggregation were taken with an Innova AFM (Bruker, Santa Barbara, CA) with a 1-10 Ohm-cm phosphorous-doped Si probe (Bruker, Part: MPP-31123-10) in contact mode with a scan rate of 0.3 Hz. Images and measurements were evaluated using Nanoscope v8.1 software.

2.3 Results and Discussion

2.3.1 Wheat gluten (WG) self-assembly with varying polypeptide concentration.

Figure 1 shows the change in morphology of WG polypeptide solutions as a function of concentration and time. No discernible morphological features were present at the onset of the experiment. As time progressed, lower concentrations displayed a predominantly fibrillar morphology (Figures 2.1 a-c) and higher concentrations displayed a predominantly globular morphology (Figures 2.1d,e). Globules were always larger than fibrils, and fibrils formed at high concentration were larger than those formed at low concentration. The length of the fibrils observed increased by 4-7 µm over the time period with 15 mg/ml showing the largest increase in length and 25 mg/ml showing the smallest (Figure 2.2). Fibril formation was observed at 15 mg/ml over all time. For 25 mg/ml and 35 mg/ml, fibril formation was observed until late time when globular morphology appeared. These fibrils showed a slight increase in diameter and length over time. Globular morphology was observed in the 45 mg/ml and 55 mg/ml until late time

when fibrils were observed. The diameter of the fibrils observed at late time for 45 mg/ml and 55 mg/ml were the largest, 0.3-0.4 μm.

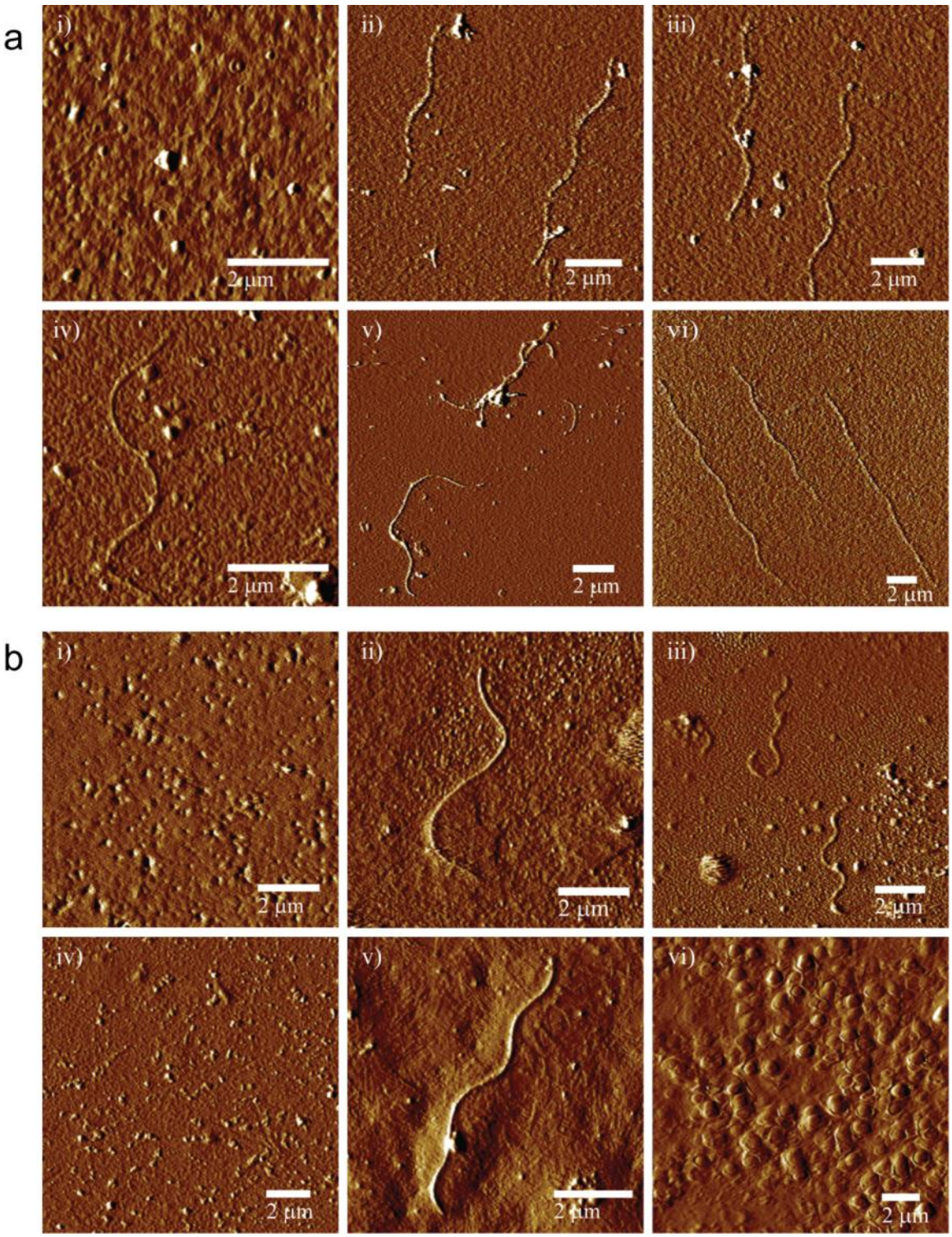

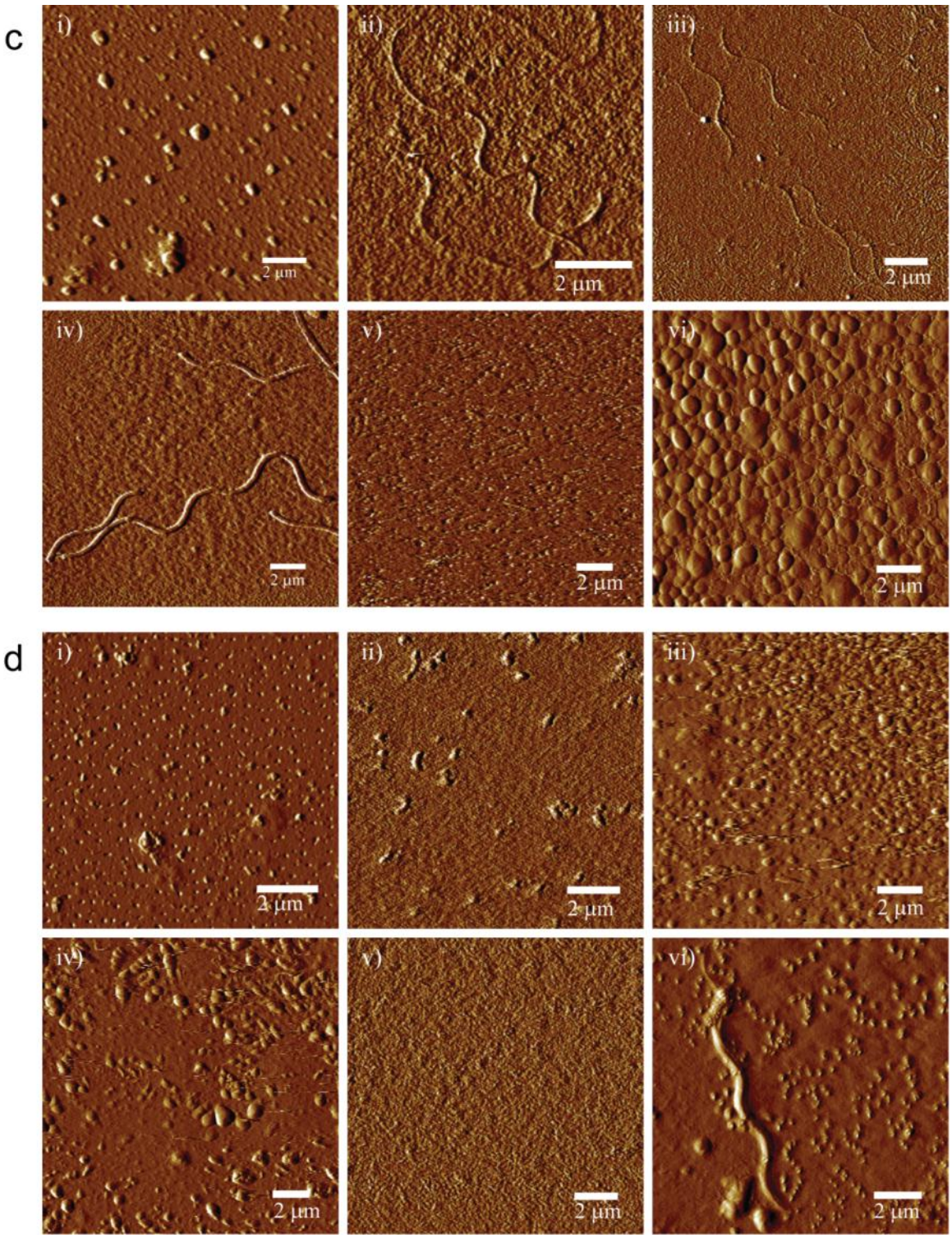
c
i)
2 µm
ii)
2 µm
iii)
2 µm
iv)
2 µm
v)
2 µm
vi)
2 µm
d
i)
2 µm
ii)
2 µm
iii)
2 µm
iv)
2 µm
v)
2 µm
vi)
2 µm

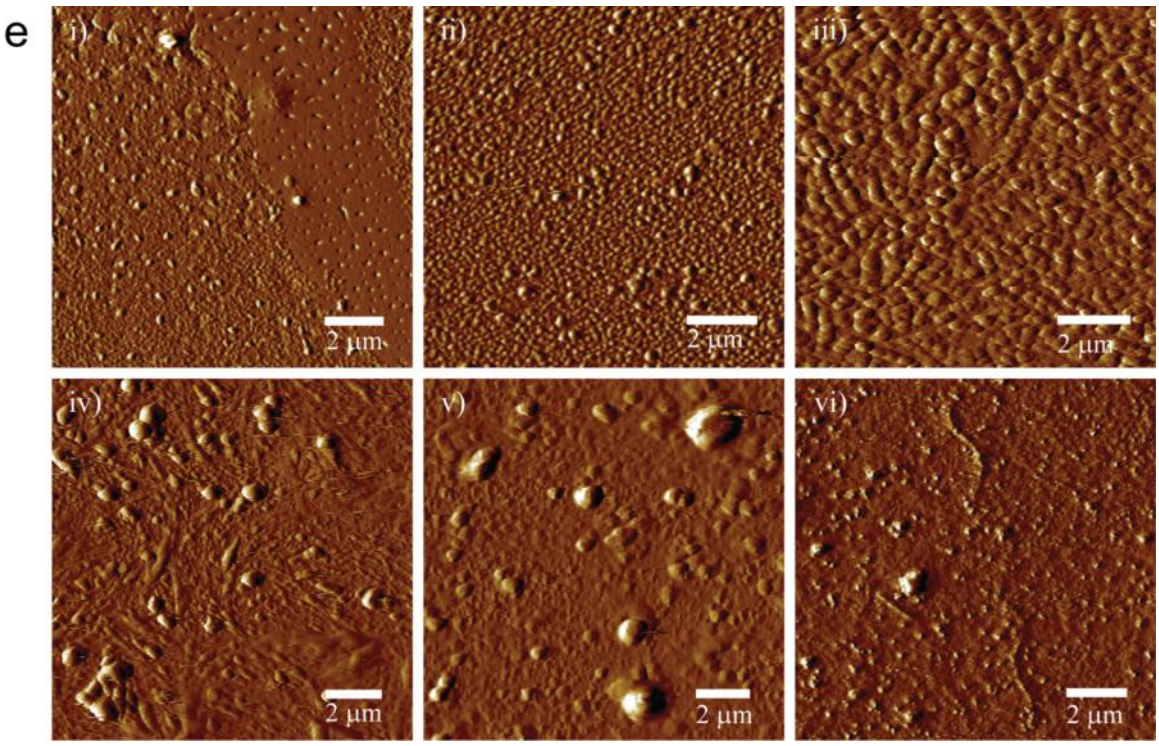

Figure 2.1 Representative AFM images of WG for concentration (a) 15mg/ml, (b) 25 mg/ml, (c) 35mg/ml, (d) 45 mg/ml, (e) 55mg/ml to show fibril/ globule formation at (i) day 0, (ii) day 4, (iii) day 8, (iv) day 12, (v) day 16, (vi) day 20. Images are deflection signal taken in tapping mode.

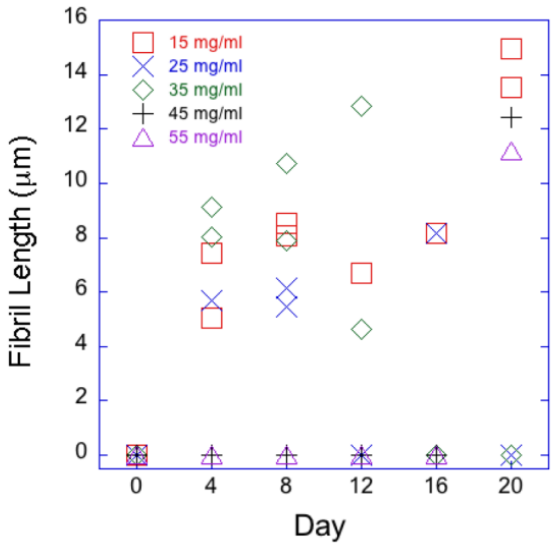

Figure 2.2 Fibril length changed over time for each concentration of WG

Self-assembly of the WG solutions was monitored over time with FTIR spectroscopy. The self-assembly process of 25 mg/ml WG solutions has been characterized with FTIR spectroscopy over a wide range of solution conditions.[55, 68, 69] It was shown that the Amide I absorbance began at 1650 cm^{-1} and then progressively decreased as the absorbance at 1610 cm^{-1} appeared and progressively increased. The contribution to Amide I at 1650 cm^{-1} was assigned to the α-helix secondary structure while that at 1610 cm^{-1} was assigned to the β-sheet secondary structure.[40, 68, 71, 74, 77, 79-89] α to β transitions are often observed in amyloid formation.[32, 90-92] Consistent with other amyloid studies, the Amide I absorbance maximum shifted from 1640-1650 cm^{-1} at 0 hr to 1610-1620 cm^{-1} at 480 hr (Figure 2.3) as aggregation progressed.[55, 69] Amyloids typically show a β-sheet Amide I position at lower wavenumber (<1620 cm^{-1}) than for native β-sheets found, for instance, in silk (~1620-1630 cm^{-1}).[93, 94] The difference does not arise from the amount of β-sheet or the ratio of anti-parallel to parallel β-sheet but differences in the β-sheet twist angle and number of protein chains or "strands" per β-sheet.[57, 95] Thus, WG yielded high strand density β-sheets typical of amyloids. The Amide I absorbance was deconvoluted and the overall change in the 1610 cm^{-1} absorbance was taken as the gain in β-sheet with time and was plotted as a function of polypeptide concentration in solution (Figure 2.4a). After 20 days of incubation, the solutions were dried and examined in the solid state using FTIR spectroscopy. The β-sheet content upon drying showed a similar trend to the overall change in high strand β-sheet content in solution (Figure 2.4b). At the same conditions, 55 mg/ml of WG produced a globular morphology of higher β-sheet content (as measured with FTIR) than the fibrils produced at 15 mg/ml.

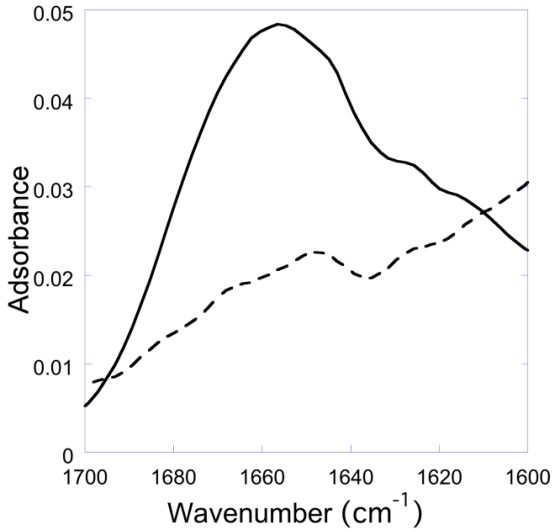

Figure 2.3 FTIR representation of WG 25 mg/ml that shows Amide I absorbance maximum shifted from 1640-1650 cm^{-1} at 0 hr (solid line) to 1610- 1620 cm^{-1} at 480 hr (dashed line). This trend is consistent with amyloid aggregation.

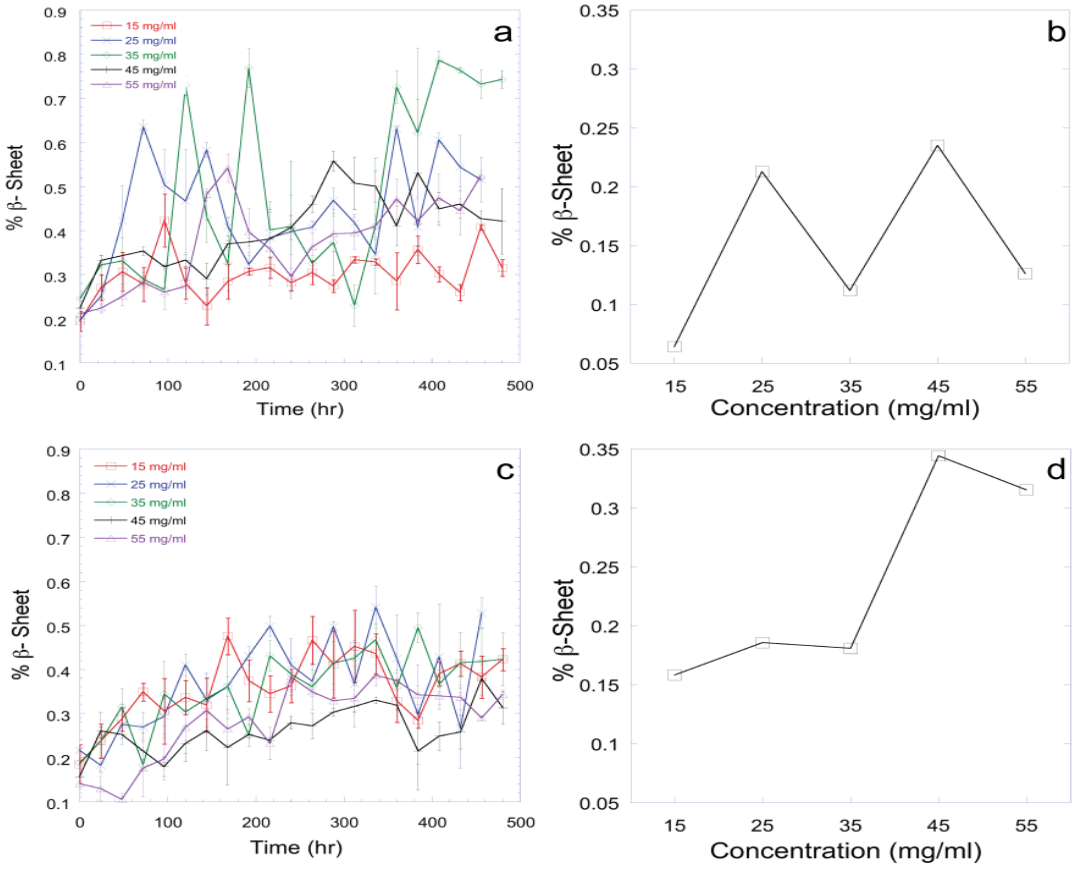

Figure 2.4 β-sheet content was determined from deconvolution of the Amide I absorbance observed with FTIR for concentration studies of (a) WG in solution (b) dried WG solutions (c) Gd:My in solution and (d) dried Gd:My solutions. There are similar trends between the liquid and dried solutions for each system.

Other changes in the FTIR spectrum were also observed. Wheat gluten is a combination of hydrolyzed gliadin (Gd, UniProt P04721, 0.49 mole fraction) and high and low molecular weight glutenin, GtH (UniProt P08488, 0.06 mole fraction) and GtL (UniProt P10386, 0.45 mole fraction), respectively, polypeptides. WG polypeptides contain significant amounts of alanine (A), isoleucine (I), leucine (L), and valine (V), which all have CH_3 side groups. Most of these side groups are contained within α-helices as determined by protein secondary structure analysis using PSIPRED.[55, 69] The up and down movement of the CH_3 side group can be defined by the symmetric CH_3 deformation, $\delta_s(CH_3)$, at 1365 cm^{-1} and the side to side movement by the asymmetric CH_3 deformation, $\delta_{as}(CH_3)$, at 1410 cm^{-1}.[79, 96, 97] Thus, if the ratio $\delta_s(CH_3)/\delta_{as}(CH_3)$ increases, CH_3 groups are laterally constrained and this defines "hydrophobic packing" as interdigitation of CH_3 groups.[55, 69, 98] The FT-IR spectrum also reveals changes in the 950-1150 cm^{-1} region. The absorbance around 1080 cm^{-1} can be assigned to the CN stretching absorbance, ν(CN), and the absorbance around 1103 cm^{-1} can be assigned to the rocking and wagging of NH_2, $\gamma_{r,w}(NH_2)$, both on amino acid side chains.[96, 97] These assignments have been shown in the Raman spectrum[99, 100] and the similarities between the Raman and FT-IR spectra for amino acids shown directly.[101] WG polypeptides also contain a large amount of glutamine repeats or "Q-blocks" and are 38% Q overall. Glutamine contains an amide group at the end of its side group connected to the peptide bond by two CH_2 groups and the ratio $\gamma_{r,w}(NH_2)/\nu(CN)$ was used to compare the state of Q side group. Specifically, the kinetics of the $\delta_s(CH_3)/\delta_{as}(CH_3)$ and $\gamma_{r,w}(NH_2)/\nu(CN)$ ratios were used to correlate fibrillar or globular morphology (Figure 2.5 a-e). A fibrillar morphology was predominantly observed at 15, 25, and 35 mg/ml. In these solutions,

$\delta_s(CH_3)/\delta_{as}(CH_3)$ decreased and then increased and the point of increase corresponded to a transition in $\gamma_{r,w}(NH_2)/\nu(CN)$. For strong fibril former 15 mg/ml, the $\gamma_{r,w}(NH_2)/\nu(CN)$ transition occurred with the increase in $\delta_s(CH_3)/\delta_{as}(CH_3)$. At 25 mg/ml and 35 mg/ml, where some globules were observed, the $\gamma_{r,w}(NH_2)/\nu(CN)$ transition occurred just prior to the increase in $\delta_s(CH_3)/\delta_{as}(CH_3)$. A globular morphology was predominantly observed at 45 and 55 mg/ml. Globular morphology showed no increase in $\delta_s(CH_3)/\delta_{as}(CH_3)$ and the $\gamma_{r,w}(NH_2)/\nu(CN)$ transition occurred at the same point $\delta_s(CH_3)/\delta_{as}(CH_3)$ was finished decreasing. Fibrils required interdigitation of CH_3 amino acid side groups. Globules formed from more random hydrophobic interactions without interdigitation. This justifies the variation in globules sizes observed in AFM (Figure 2.1), because the random formation results in a random size distribution. Interestingly, the random hydrophobic interactions brought many polypeptides together to form more β-sheets in globules than in fibrils. High β-sheet content was not a necessary requirement for fibril formation but organized hydrophobic amino acid side groups were. The increase in $\gamma_{r,w}(NH_2)/\nu(CN)$ at the transition may suggest that hydrogen bonding of the C=O on the end of the glutamine side chain occurred because vibration of CN was lost relative to NH_2.

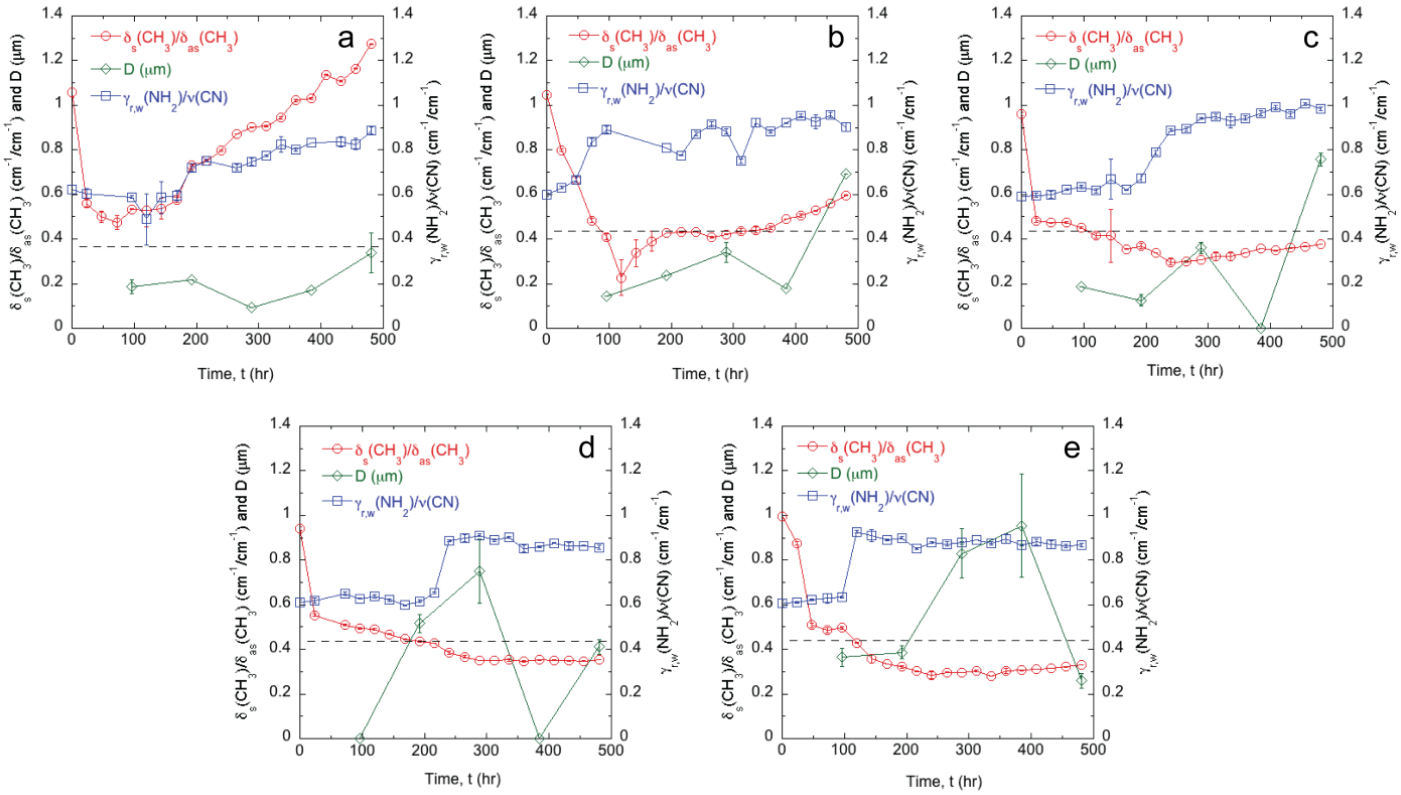

Figure 2.5 Comparison of changes in A, I, L, and V side groups versus Q side groups as determined with FTIR spectroscopy for WG system. Also shown is the fibril or globule diameter. The dashed line shows the transition from fibrils (below) to globules (above) for (a) 15mg/ml, (b) 25 mg.ml, (c) 35mg/ml, (d) 45 mg/ml, (e) 55mg/ml

2.3.2 Wheat gluten (WG) self-assembly with varying number of layers.

Polypeptide concentration was also varied by casting multiple layers of a 25 mg/ml solution at given times over the 20 day period. The shift toward a globular morphology was also observed with an increase in the number of layers. AFM data for the layering study showed similar trends to the WG studies, so Figure 2.1 is also meant to be representative of the layer study in which low concentrations showed similar trends to less layers (1 and 3) and high concentrations showed similar trends to the increased number of layers (5 and 10). During layering, there was no fibril formation on day 1 for any number of layers. At 10 layers large globules with a diameter of 3 μm appeared at day 1. Fibril formation was observed in 1 and 3 layers at later times and the diameter and

length of the fibrils was consistently 0.1-0.2 μm and 4-10 μm, respectively. In 5 and 10 layers globular morphology similar in phase to a separated polymer blend was observed at early time and fibril formation was not observed until late time. Long fibers around 9 μm were observed at 5 layers, but on the last day only short fibers, around 3 and 4 μm were observed.

The number of fibrils per scan area (μm^2) was also monitored for both the concentration and layering experiments (Figure 2.6 a and b). AFM images with areas of approximately 10 μm^2 were chosen for this procedure. For lower peptide concentration or number of layers, the number of fibrils/area was fairly consistent with time. At 35 mg/ml the number of fibrils steadily decreased over time. At 45 mg/ml and 55 mg/ml, fibrils were observed only at day 20. Interestingly, there was a stage where neither fibrils nor globules were clearly identifiable, i.e., the material just appeared to be a featureless coating. This "coating" was observed on at day 0, at day 10 for 3, 5, and 10 drops, and on day 16 for 35 mg/ml and 45 mg/ml. The featureless coating occurred between major changes in the morphology. Day 10 of the layer method was the point between observation of fibrils and observation of globules for 5 and 10 drops. For varying concentration, day 16 was the point between observation of fibrils and globules at 35 mg/ml and the opposite transition for 45 mg/ml (Figure 2.1 c v and d v).

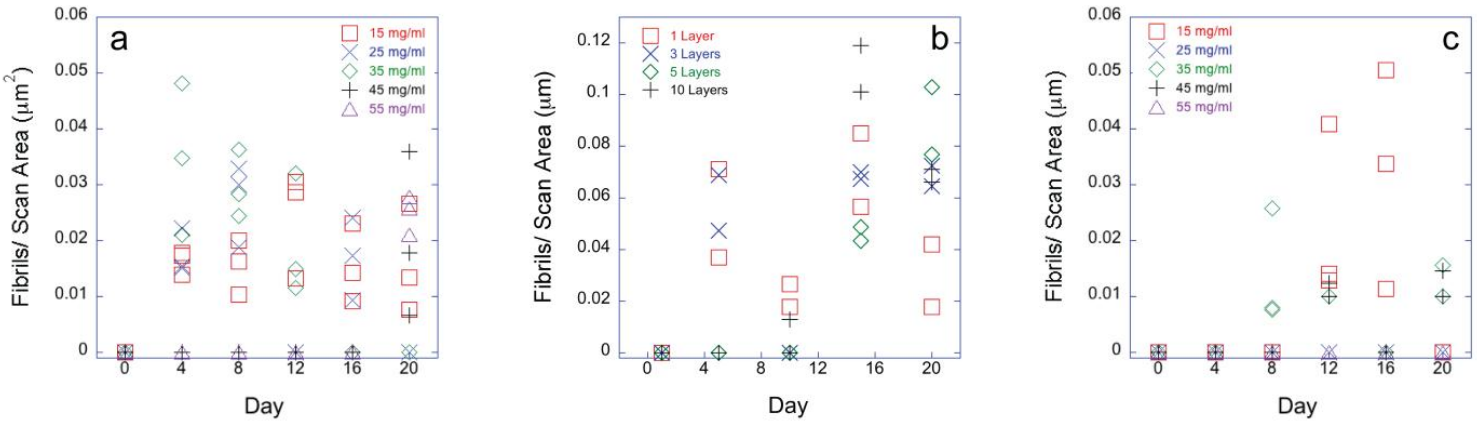

Figure 2.6 To gain a quantitative idea of the number of fibrils observed at each time point, the number of fibrils were counted for the area of the image obtained from AFM for (a) WG concentration (b) WG layers and (c) Gd:My concentration

2.3.3 Gliadin:Myoglobin (Gd:My) self-assembly with varying polypeptide concentration.

A study varying the concentration of Gd:My was performed in the same manner as the varying concentration of WG solution. A summary of the Gd:My peptide concentration behavior is shown in Figure 2.7 and the average number of fibrils/area is shown in Figure 2.6c. The behavior of this system is qualitatively similar to the WG system. Gd:My showed a fibrillar morphology over a more narrow range of time and concentration (Figures 2.7a,c,6) and the fibrils were smaller in diameter than WG fibrils. Solutions of concentration 25mg/ml and 55mg/ml showed no fiber formation and only minor globular formation. Globules and fibrils were more similar in diameter than observed in WG solutions. The aggregation patterns observed in Figure 2.7 b v and Figure 2.7 c v are thought to be attributed to glutamine crystallization. Gd:My does contain glutamine, although in reduced quantities compared to WG and this pattern has been observed in other systems that contain glutamine.

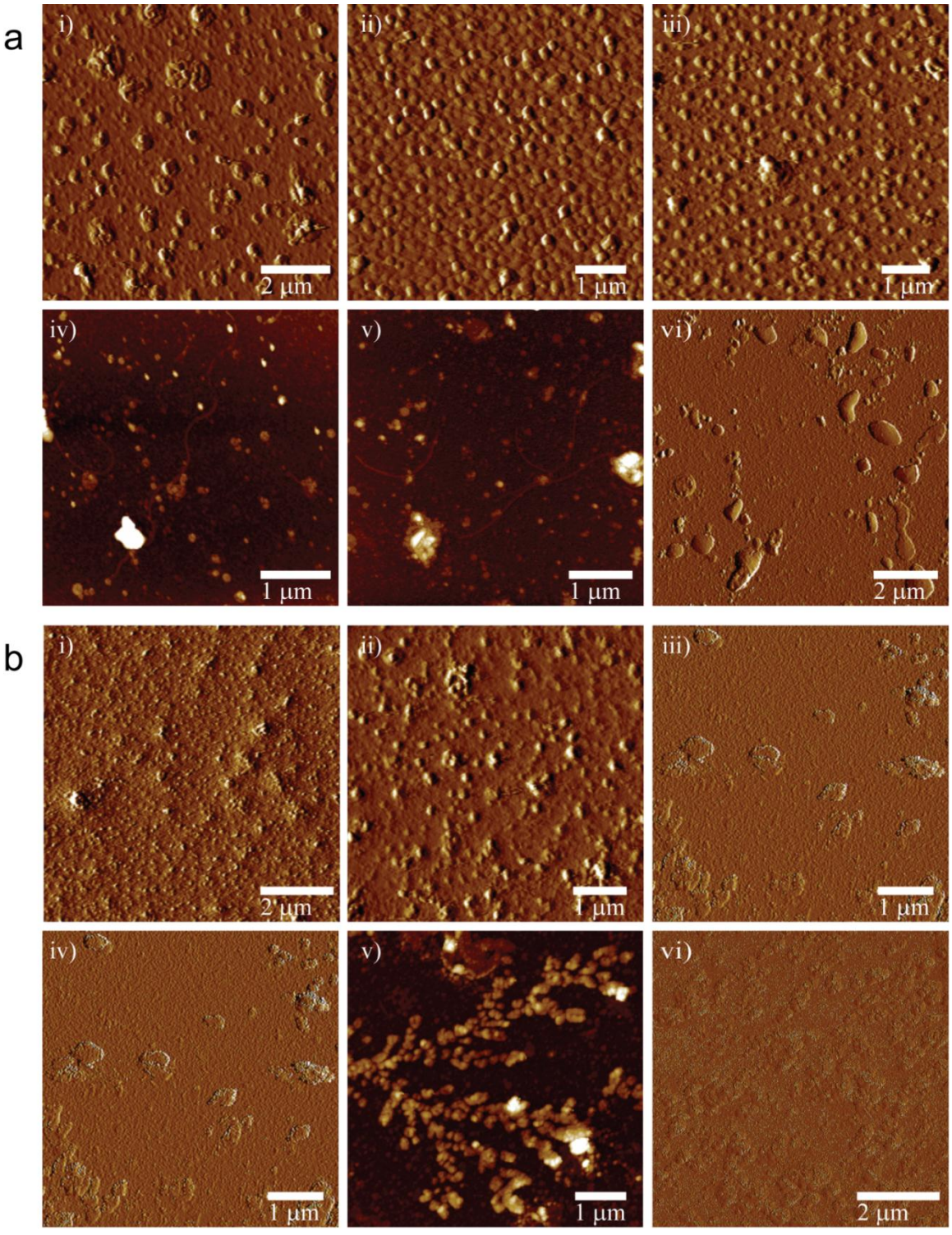
a
i)
2 µm
ii)
1 µm
iii)
1 µm
iv)
1 µm
v)
1 µm
vi)
2 µm
b
i)
2 µm
ii)
1 µm
iii)
1 µm
iv)
1 µm
v)
1 µm
vi)
2 µm

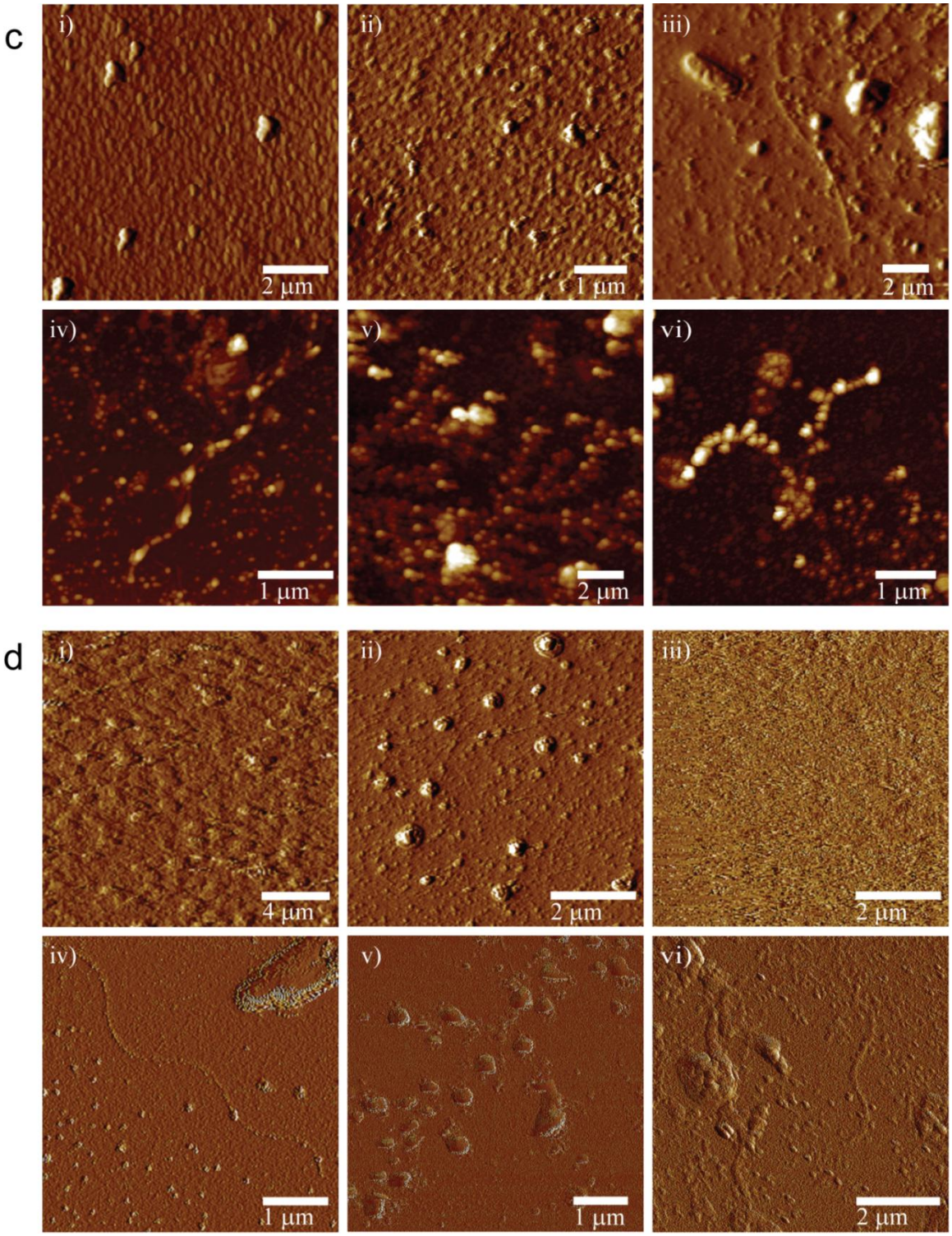
c
i)
2 µm
ii)
1 µm
iii)
2 µm
iv)
1 µm
v)
2 µm
vi)
1 µm
d
i)
4 µm
ii)
2 µm
iii)
2 µm
iv)
1 µm
v)
1 µm
vi)
2 µm

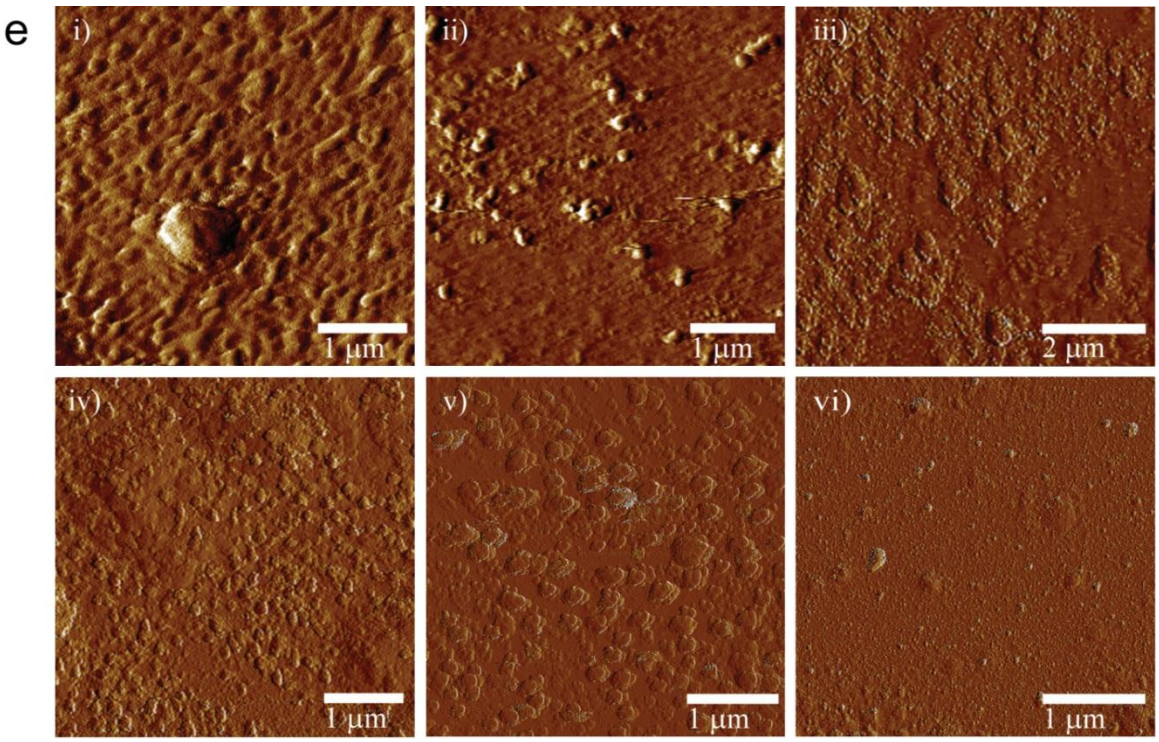

Figure 2.7 Representative AFM images of Gd-My for concentration (a) 15mg/ml, (b) 25 mg.ml, (c) 35mg/ml, (d) 45 mg/ml, (e) 55mg/ml to show fibril/ globule formation at day (i) day 0, (ii) day 4, (iii) day 8, (iv) day 12, (v) day 16, (vi) day 20. Images are either height or tapping phase taken in contact mode.

FTIR spectroscopy has also been used to study the self-assembly of 25 mg/ml Gd:My solutions.[55, 69] The same procedures used to characterize WG were also used to characterize Gd:My. The Amide I absorbance was also deconvoluted and the overall change in the 1610 cm^{-1} absorbance was taken as the gain in β-sheet with time and was plotted as a function of polypeptide concentration in solution (Figure 2.4c). After 20 days of incubation, the solutions were dried and examined in the solid state using FTIR spectroscopy. The β-sheet content upon drying showed differences compared to the overall change β-sheet content in solution (Figure 2.4d). After drying, 45 mg/ml and 55 mg/ml showed the highest β-sheet content, whereas in solution they showed a lower percentage than the other concentrations.

The same kinetics of the $\delta_s(CH_3)/\delta_{as}(CH_3)$ and $\gamma_{r,w}(NH_2)/\nu(CN)$ ratios that were used to correlate fibrillar and globular morphology for WG were also used with the Gd:My system (Figure 2.8 a-e). In WG, the ratio $\gamma_{r,w}(NH_2)/\nu(CN)$ was used to compare the state of the Q side group. The amount of Q blocks are significantly reduced in Gd:My, therefore the $\gamma_{r,w}(NH_2)/\nu(CN)$ ratio remained relatively consistent at 0.8 and only slightly mimicked the trends of the $\delta_s(CH_3)/\delta_{as}(CH_3)$ ratio. There were no strong fibril forming systems like in WG, but the ratios showed similar trends to the WG system. A fibrillar morphology was observed over a more narrow range of time for concentrations of 15, 35, and 45 mg/ml. In these solutions, sharp $\delta_s(CH_3)/\delta_{as}(CH_3)$ decreases usually corresponded with fibril formation. For these systems and 25 mg/ml there was an inverse relationship between the $\delta_s(CH_3)/\delta_{as}(CH_3)$ ratio and globule diameter overtime. The 55mg/ml which only exhibited globules at one time point showed a steady increase in the $\delta_s(CH_3)/\delta_{as}(CH_3)$ ratio. The trends in the $\delta_s(CH_3)/\delta_{as}(CH_3)$ are similar between the concentration studies of WG and Gd:My and fibrils were observed in both systems. It can therefore be concluded interdigitation of the CH_3 groups is a necessity for fibril formation and that glutamine amide hydrogen bonding is not a necessity but aids in the process because fibrils observed in the WG system were larger and more abundant.

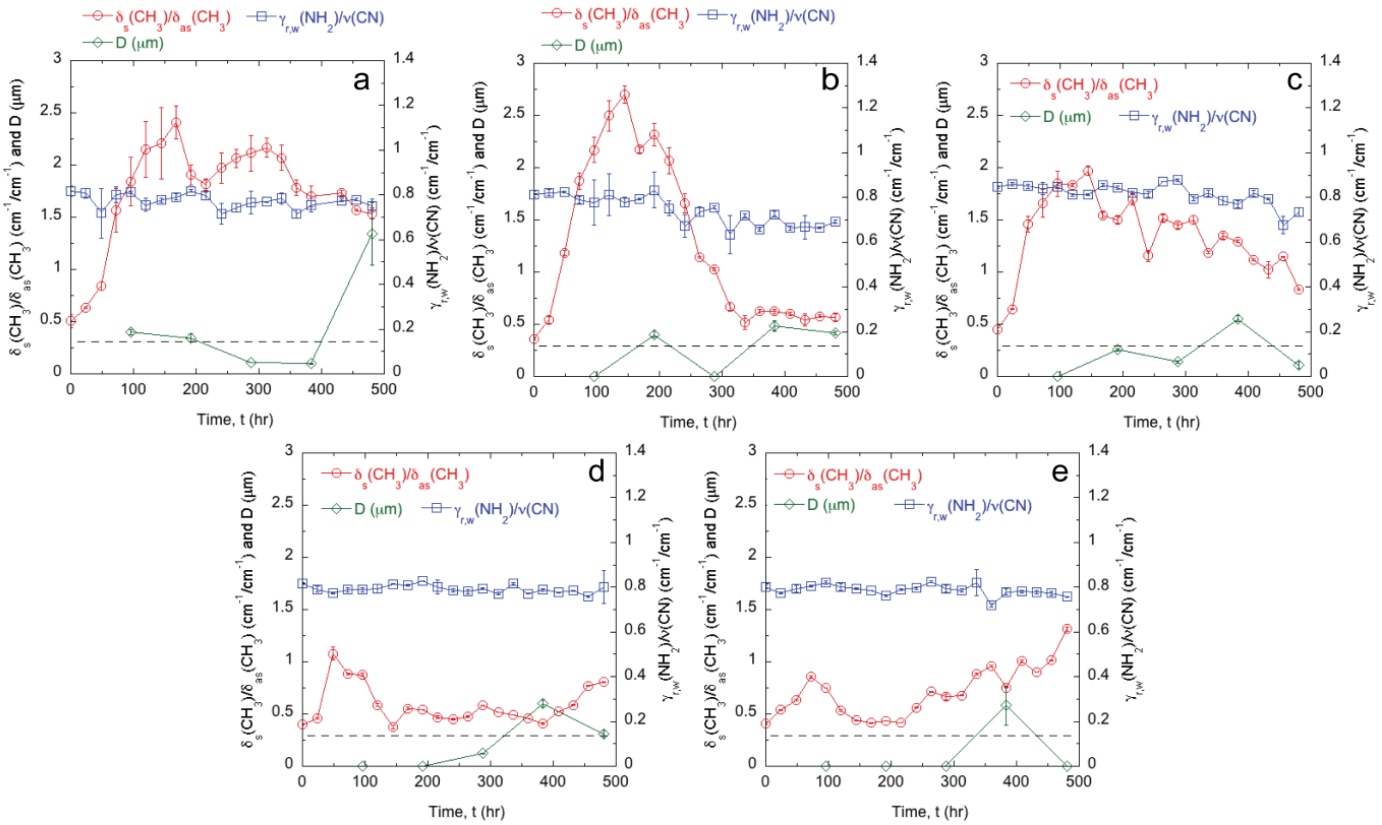

Figure 2.8 Comparison of changes in A, I, L, and V side groups versus Q side groups as determined with FTIR spectroscopy for the Gd:My system. Also shown is the fibril or globule diameter. The dashed line shows the transition from fibrils (below) to globules (above) for (a) 15mg/ml, (b) 25 mg.ml, (c) 35mg/ml, (d) 45 mg/ml, (e) 55mg/ml

2.4 Conclusion

We have shown that it is possible to control the morphology of amyloid structures using concentration. Lower polypeptide concentrations and fewer layers produced fibrils while higher ones produced globules. Fibrils had lower β-sheet content than globules. Fibrils required interdigitation of CH_3 groups on A, I, L, and V that occur concurrently with glutamine amide hydrogen bonding. Globules formed from more random hydrophobic interactions that preceded glutamine amide hydrogen bonding. The ability to control when and where the different types of morphologies occur could be beneficial for engineering future materials with specific properties related to the morphology. In

terms of barnacles, an interesting hypothesis is whether a self-assembled amyloid coating similar to barnacle adhesive could act as an antifouling coating. This self-assembled protein coating would be at equilibrium and would therefore discourage barnacle proteins introduced by the organism to further self-assemble and attach to the surface.

Acknowledgements

Generous funding through NSF-CMMI-0856262 and the Virginia Tech Biodesign and Bioprocessing Research Center are greatly appreciated.

References

1. Dobson, C. M., Protein misfolding, evolution and disease. *Trends in Biochemical Science* **1999,** 24, 329-332.

2. Dobson, C. M., Sali,A. and Darplus,M., Protein folding: a perspective from theory and experiment. *Angew. Chem (Int. Ed.)* **1998,** 37.

3. Chiti, F.; Dobson, C. M., Protein misfolding, functional amyloid, and human disease. *Annual review of biochemistry* **2006,** 75, 333-66.

4. Dobson, C. M., Protein folding and misfolding. *Nature* **2003,** 426, 884-890.

5. Prusiner, S. B., Prions. *Proceedings of the National Academy of Sciences* **1998,** 95, (23), 13363-13383.

6. Bouchard, M.; Zurdo, J.; Nettleton, E. J.; Dobson, C. M.; Robinson, C. V., Formation of insulin amyloid fibrils followed by FTIR simultaneously with CD and electron microscopy. *Protein Science* **2000,** 9, 1960-1967.

7. Chen, S.; Berthelier, V.; Bradley Hamilton, J.; O'Nuallain, B.; Wetzel, R., Amyloid-like features of polyglutamine aggregates and their assembly kinetics. *Biochemistry* **2002,** 41, 7391-7399.

8. Cherny, I.; Gazit, E., Amyloids: Not only pathological agents but also ordered nanomaterials. *Angewandte Chemie International Edition* **2008,** 47, (22), 4062-4069.

9. Cohen, A. S.; Calkins, E., Electron microscopic observations on a fibrous component in amyloid of diverse origins. *Nature* **1959,** 183, 1202-1203.

10. del Mercato, L. L.; Maruccio, G.; Pompa, P. P.; Bochiccio, B.; Tamburro, A. M.; Cingolani, R.; Rinaldi, R., Amyloid-like fibrils in elastin-related polypeptides: Structural characterization and elastic properties. *Biomacromolecules* **2008,** 9, (3), 796-803.

11. Diaz-Avalos, R., Cross-β order and diversity in nanocrystals of an amyloid-forming peptide. *J. Mol. Biol.* **2003,** 330, 1165-1175.

12. Eanes, E. D.; Glenner, G. G., X-ray diffraction studies on amyloid filaments. *J. Histochem. Cytochem.* **1968,** 16, 673-677.

13. Gosal, W. S.; Clark, A. H.; Pudney, P. D. A.; Ross-Murphy, S. B., Novel amyloid fibrillar networks derived from a globular protein: β-lactoglobulin. *Langmuir* **2002,** 18, (19), 7174-7181.

14. Ivanova, M. I.; Sawaya, M. R.; Gingery, M.; Attinger, A.; Eisenberg, D., An amyloid-forming segment of β2-microglobulin suggests a molecular model for the fibril. *Proc. Natl Acad. Sci. USA* **2004,** 101, 10584-10589.

15. Jaroniec, C. P.; MacPhee, C. E.; Astrof, N. S.; Dobson, C. M.; Griffin, R. G., Molecular conformation of a peptide fragment of transthyretin in an amyloid fibril. *Proc. Natl Acad. Sci. USA* **2002,** 99, 16748-16753.

16. Jimenez, J. L., Cryo-electron microscopy structure of an SH3 amyloid fibril and model of the molecular packing. *EMBO J.* **1999,** 18, 815-821.

17. Jimenez, J. L., The protofilament structure of insulin amyloid fibrils. *Proc. Natl Acad. Sci. USA* **2002,** 99, 9196-9201.

18. MacPhee, C. E.; Dobson, C. M., Formation of mixed fibrils demonstrates the generic nature and potential utility of amyloid nanostructures. *Journal of the American Chemical Society* **2000,** 122, 12707-12713.

19. Pearce, F. G.; Mackintosh, S. H.; Gerrard, J. A., Formation of amyloid-like fibrils by ovalbumin and related proteins under conditions relevant to food processing. *Journal of Agricultural and Food Chemistry* **2007,** 55, 318-322.

20. Perutz, M. F.; Finch, J. T.; Berriman, J.; Lesk, A., Amyloid fibers are water-filled nanotubes. *Proc. Natl Acad. Sci. USA* **2002,** 99, 5591-5595.

21. Petkova, A. T., A structural model for Alzheimer's β-amyloid fibrils based on experimental constraints from solid state NMR. *Proc. Natl Acad. Sci. USA* **2002,** 99, 16742-16747.

22. Rubin, N.; Perugia, E.; Goldschmidt, M.; Fridkin, M.; Addadi, L., Chirality of amyloid suprastructures. *Journal of the American Chemical Society* **2008,** 130, 4602-4603.

23. Scheibel, T.; Parthasarathy, R.; Sawicki, G.; Lin, X.-M.; Jaeger, H.; Lindquist, S. L., Conducting nanowires built by controlled self-assembly of amyloid fibers and selective metal deposition. *Proceedings of the National Academy of Sciences* **2003,** 100, 4527-4532.

24. Sunde, M.; Blake, C. C. F., From the globular to the fibrous state: protein structure and structural conversion in amyloid formation. *Quarterly Reviews of Biophysics* **1998,** 31, (1), 1-39.

25. Torok, M., Structural and dynamic features of Alzheimer's Aβ peptide in amyloid fibrils studied by site-directed spin labeling. *J. Biol. Chem.* **2002,** 277, 40810-40815.

26. Zurdo, J.; Guijarro, J. I.; Dobson, C. M., Preparation and characterization of purified amyloid fibrils. *Journal of the American Chemical Society* **2001,** 123, 8141-8142.

27. Adamcik, J.; Berquand, A.; Mezzenga, R., Single-step direct measurement of amyloid fibrils stiffness by peak force quantitative nanomechanical atomic force microscopy. *Applied Physics Letters* **2011,** 98, 193701.

28. Adamcik, J.; Jung, J.-M.; Flakowski, J.; De Los Rios, P.; Dietler, G.; Mezzenga, R., Understanding amyloid aggregation by statistical analysis of atomic force microscopy images. *Nat Nano* **2010,** 5, (6), 423-428.

29. Adamcik, J.; Mezzenga, R., Adjustable twisting periodic pitch of amyloid fibrils. *Soft Matter* **2011,** 7, (11), 5437-5443.

30. Bolder, S. G.; Hendrickx, H.; Sagis, L. M. C.; van der Linden, E., Fibril assemblies in aqueous whey protein mixtures. *Journal of Agricultural and Food Chemistry* **2006,** 54, 4229-4234.

31. Bolisetty, S.; Adamcik, J.; Mezzenga, R., Snapshots of fibrillation and aggregation kinetics in multistranded amyloid β-lactoglobulin fibrils. *Soft Matter* **2011,** 7, 493-499.

32. Fandrich, M.; Forge, V.; Buder, K.; Kittler, M.; Dobson, C. M.; Diekmann, S., Myoglobin forms amyloid fibrils by association of unfolded polypeptide segments. *Proceedings of the National Academy of Sciences* **2003,** 100, (26), 15463-15468.

33. Goda, S.; Takano, K.; Yamagata, Y.; Nagata, R.; Akutsu, H.; Maki, S.; Namba, K.; Yutani, K., Amyloid protofilament formation of hen egg lysozyme in highly concentrated ethanol solution. *Protein Science* **2000,** 9, 369-375.

34. Mostaert, A.; Higgins, M. J.; Fukuma, T.; Rindi, F.; Jarvis, S. P., Nanoscale mechanical characterization of amyloid fibrils discovered in a natural adhesive. *Journal of Biological Physics* **2006,** 32, 393-401.

35. Aggeli, A.; Nyrkova, I. A.; Bell, M.; Harding, R.; Carrick, L.; McLeish, T. C. B.; Semenov, A. N.; Boden, N., Hierarchical self-assembly of chiral rod-like molecules as a

model for peptide β-sheet tapes, ribbons, fibrils, and fibers. *Proceedings of the National Academy of Sciences* **2001,** 98, (21), 11857-11862.

36. Davies, R. P. W.; Aggeli, A.; Beevers, A. J.; Boden, N.; Carrick, L. M.; Fishwick, C. W. G.; McLeish, T. C. B.; Nyrkova, I. A.; Semenov, A. N., Self-assembling β-sheet tape forming peptides. *Supramolecular Chemistry* **2006,** 18, (5), 435-443.

37. Nyrkova, I. A.; Semenov, A. N.; Aggeli, A.; Bell, M.; Boden, N.; McLeish, T. C. B., Self-assembly and structure formation in living polymers forming fibrils. *European Physical Journal B* **2000,** 17, 499-513.

38. Nyrkova, I. A.; Semenov, A. N.; Aggeli, A.; Boden, N., Fibril stability in solutions of twisted β-sheet peptides: a new kind of micellization in chiral systems. *European Physical Journal B* **2000,** 17, 481-497.

39. Parker, K. D.; Rudall, K. M., Structure of the silk of *Chrysopa* egg-stalks. *Nature* **1957,** 179, 905-906.

40. Fraser, R. D. B.; MacRae, T. P., *Conformation in Fibrous Proteins and Related Synthetic Polypeptides*. Academic Press: New York, 1973.

41. Jin, H.-J.; Kaplan, D. L., Mechanism of silk processing in insects and spiders. *Nature* **2003,** 424, 1057-1061.

42. Knowles, T. P. J.; Buehler, M. J., Nanomechanics of functional and pathological amyloid materials. *Nat Nano* **2011,** 6, (8), 469-479.

43. Fowler, D. M.; Koulov, A. V.; Balch, W. E.; Kelly, J. W., Functional amyloid-From bacteria to humans. *TRENDS in Biochemical Sciences* **2007,** 32, (5), 217-224.

44. Barlow, D. E.; Dickinson, G. H.; Orihuela, B.; Kulp, J. L.; Rittschof, D.; Wahl, K. J., Characterization of the Adhesive Plaque of the Barnacle Balanus amphitrite: Amyloid-Like Nanofibrils Are a Major Component. *Langmuir* **2010,** 26, (9), 6549-6556.

45. Kamino, K.; Odo, S.; Maruyama, T., Cement Proteins of the Acorn-Barnacle, Megabalanus rosa. *The Biological Bulletin* **1996,** 190, (3), 403-409.

46. Kamino, K.; Inoue, K.; Maruyama, T.; Takamatsu, N.; Harayama, S.; Shizuri, Y., Barnacle cement proteins. *Journal of Biological Chemistry* **2000,** 275, (35), 27360-27365.

47. Sullan, R. M. A.; Gunari, N.; Tanur, A. E.; Chan, Y.; Dickinson, G. H.; Orihuela, B.; Rittschof, D.; Walker, G. C., Nanoscale structures and mechanics of barnacle cement. *Biofouling* **2009,** 25, (3), 263-275.

48. Gebbink, M. F. B. G.; Claessen, D.; Bouma, B.; Dijkhuizen, L.; Wosten, H. A. B., Amyloids-A functional coat for microorganisms. *Nature Reviews Microbiology* **2005,** 3, 333-341.

49. Ben Nasr, A.; Olsen, A.; Sjobring, U.; Muller-Esterl, W.; Bjorck, L., Assembly of human contact phase proteins and release of bradykinin at the surface of curli-expressing *Escheria coli*. *Molecular Microbiology* **1996,** 20, (5), 927-935.

50. Hammer, N. D.; Schmidt, J. C.; Chapman, M. R., The curli nucleator protein, CsgB, contains an amyloidogenic domain that directs CsgA polymerization. *Proceedings of the National Academy of Sciences* **2007,** 104, (30), 12494-12499.

51. Wang, X.; Chapman, M. R., Curli provide the template for understanding controlled amyloid propagation. *Prion* **2008,** 2, (2), 57-60.

52. Parker, K. D.; Rudall, K. M., The silk of the egg-stalk of the green lace-wing fly. *Nature* **1957,** 179, 905-906.

53. Weisman, S.; Trueman, H. E.; Mudie, S. T.; Church, J. S.; Sutherland, T. D.; Haritos, V. S., An unlikely silk: The composite material of green lacewing cocoons. *Biomacromolecules* **2008,** 9, (11), 3065-3069.

54. Keten, S.; Buehler, M. J., Nanostructure and molecular mechanics of spider dragline silk protein assemblies. *Journal of The Royal Society Interface* **2010,** 7, (53), 1709-1721.

55. Ridgley, D. M.; Ebanks, K. C.; Barone, J. R., Peptide mixtures can self-assemble into large amyloid fibers of varying size and morphology. *Biomacromolecules* **2011,** 12, (10), 3770-3779.

56. Paparcone, R.; Buehler, M. J., Microscale structural model of Alzheimer Aβ(1-40) amyloid fibril. *Applied Physics Letters* **2009,** 94, (24), 243904-3.

57. Paparcone, R.; Keten, S.; Buehler, M. J., Atomistic simulation of nanomechanical properties of Alzheimer's Aβ(1-40) amyloid fibrils under compressive and tensile loading. *Journal of Biomechanics* **2010,** 43, 1196-1201.

58. Seidel, A.; Liivak, O.; Calve, S.; Adaska, J.; Ji, G.; Yang, Z.; Grubb, D.; Zax, D. B.; Jelinski, L. W., Regenerated spider silk: Processing, properties, and function. *Macromolecules* **2000,** 33, (3), 775-780.

59. Fukuma, T.; Mostaert, A.; Jarvis, S., Explanation for the mechanical strength of amyloid fibrils. *Tribology Letters* **2006,** 22, (3), 233-237.

60. Knowles, T. P. J.; Oppenheim, T. W.; Buell, A. K.; Chirgadze, D. Y.; Welland, M. E., Nanostructured films from hierarchical self-assembly of amyloidogenic proteins. *Nat Nano* **2010,** 5, (3), 204-207.

61. Power, A. M.; Klepal, W.; Zheden, V.; Jonker, J.; McEvilly, P.; Byern, J., Mechanisms of Adhesion in Adult Barnacles

Biological Adhesive Systems. In Byern, J.; Grunwald, I., Eds. Springer Vienna: 2010; pp 153-168.

62. Dickinson, G. H.; Vega, I. E.; Wahl, K. J.; Orihuela, B.; Beyley, V.; Rodriguez, E. N.; Everett, R. K.; Bonaventura, J.; Rittschof, D., Barnacle cement: a polymerization model based on evolutionary concepts. *Journal of Experimental Biology* **2009,** 212, (21), 3499-3510.

63. Vincent, J., *Structural Biomaterials*. Princeton University Press: Princeton, 1990.

64. Rzepecki, L. M.; Waite, J. H., Wrestling the muscle from mussel beards: research and applications. *Molecular Marine Biology and Biotechnology* **1995,** 3, 313-322.

65. Brazee, S. L.; Carrington, E., Interspecific Comparison of the Mechanical Properties of Mussel Byssus. *The Biological Bulletin* **2006,** 211, (3), 263-274.

66. Wiegemann, M.; Watermann, B., Peculiarities of barnacle adhesive cured on non-stick surfaces. *Journal of Adhesion Science and Technology* **2003,** 17, (14), 1957-1977.

67. Berglin, M.; Gatenholm, P., The barnacle adhesive plaque: morphological and chemical differences as a response to substrate properties. *Colloids and Surfaces B: Biointerfaces* **2003,** 28, (2–3), 107-117.

68. Athamneh, A.; Barone, J. R., Enzyme-mediated self-assembly of highly ordered structures from disordered proteins. *Smart Materials and Structures* **2009,** 18, 104024 (8pp).

69. Ridgley, D. M.; Claunch, E. C.; Barone, J. R., The effect of processing on large, self-assembled amyloid fibers. *Soft Matter* **2012,** 8, (40), 10298-10306.

70. Ridgley, D. M.; Barone, J. R., Evolution of the amyloid fiber over multiple length scales. *ACS Nano* **2013,** DOI: 10.1021/nn303489a.

71. Krimm, S.; Bandekar, J., Vibrational spectroscopy and conformation of peptides, polypeptides, and proteins. In *Advances in Protein Chemistry*, Anfinsen, C. B.; Edsall, J. T.; Richards, F. M., Eds. Academic Press, Inc.: Orlando, 1986; Vol. 38, pp 181-364.

72. Byler, D. M.; Susi, H., Examination of the secondary structure of proteins by deconvolved FTIR spectra. *Biopolymers* **1986,** 25, (3), 469-487.

73. Arrondo, J. L. R.; Muga, A.; Castresana, J.; Goñi, F. M., Quantitative studies of the structure of proteins in solution by Fourier-transform infrared spectroscopy. *Progress in Biophysics and Molecular Biology* **1993,** 59, (1), 23-56.

74. Vecchio, G.; Bossi, A.; Pasta, P.; Carrea, G., Fourier-transform infrared conformational study of bovine insulin in surfactant solutions. *International Journal of Peptide and Protein Research* **1996,** 48, (2), 113-117.

75. Surewicz, W. K.; Mantsch, H. H.; Chapman, D., Determination of protein secondary structure by Fourier transform infrared spectroscopy: A critical assessment. *Biochemistry* **1993,** 32, (2), 389-394.

76. Susi, H.; Byler, D. M., Resolution-enhanced fourier transform infrared spectroscopy of enzymes. In *Methods in Enzymology*, C. H. W. Hirs, S. N. T., Ed. Academic Press: 1986; Vol. Volume 130, pp 290-311.

77. Surewicz, W. K.; Mantsch, H. H., New insight into protein secondary structure from resolution-enhanced infrared spectra. *Biochimica et Biophysica Acta* **1988,** 952, 115-130.

78. Bradley, M., Curve fitting in Raman and IR spectroscopy: Basic theory of line shapes and applications. In Thermo Fisher Scientific, I., Ed. Thermo Fisher Scientific, Inc.: Madison, 2007; Vol. 50733.

79. Miyazawa, T.; Shimanouchi, T.; Mizushima, S.-i., Characteristic Infrared Bands of Monosubstituted Amides. *The Journal of Chemical Physics* **1956,** 24, (2), 408-418.

80. Blout, E. R.; Idelson, M., Polypeptides. VI. Poly-α-L-glutamic acid: Preparation and helix-coil conversion. *Journal of the American Chemical Society* **1956,** 78, 497-498.

81. Lenormant, H.; Baudras, A.; Blout, E. R., Reversible configurational changes in sodium poly-α-L-glutamate induced by water. *Journal of the American Chemical Society* **1958,** 80, 6191-6195.

82. Fraser, R. D. B.; Harrap, B. S.; MacRae, T. P.; Stewart, F. H. C.; Suzuki, E., Effect of glycyl residues on the stability of the α-helix. *Biopolymers* **1967,** 5, 221-257.

83. Nevskaya, N. A.; Chirgadze, Y. N., Infrared spectra and resonance interactions of amide-I and II vibrations of α-helix. *Biopolymers* **1976,** 15, (4), 637-648.

84. Vendantham, G.; Sparks, H. G.; Sane, S. U.; Tzannis, S.; Przybycien, T. M., A holistic approach for protein secondary structure estimation from infrared spectra in H_2O solutions. *Analytical Biochemistry* **2000,** 285, 33-49.

85. Goormaghtigh, E.; Cabiaux, V.; Ruysschaert, J.-M., Secondary structure and dosage of soluble and membrane proteins by attenuated total reflection Fourier-transform infrared spectroscopy on hydrated films. *European Journal of Biochemistry* **1990,** 193, (2), 409-420.

86. Kumosinski, T. F.; Unruh, J. J., Quantitation of the global secondary structure of globular proteins by FTIR spectroscopy: Comparison with X-ray crystallographic structure. *Talanta* **1996,** 43, (2), 199-219.

87. Balbirnie, M.; Grothe, R.; Eisenberg, D. S., An amyloid-forming peptide from the yeast prion Sup35 reveals a dehydrated β-sheet structure for amyloid. *Proceedings of the National Academy of Sciences* **2001,** 98, (5), 2375-2380.

88. Halverson, K.; Fraser, P. E.; Kirschner, D. A.; Lansbury, P. T., Molecular determinants of amyloid deposition in Alzheimer's disease: conformational studies of synthetic β-protein fragments. *Biochemistry* **1990,** 29, (11), 2639-2644.

89. Bouchard, M.; Zurdo, J.; Nettleton, E. J.; Dobson, C. M.; Robinson, C. V., Formation of insulin amyloid fibrils followed by FTIR simultaneously with CD and electron microscopy. *Protein Science* **2000,** 9, (10), 1960-1967.

90. Fandrich, M.; Fletcher, M. A.; Dobson, C. M., Amyloid fibrils from muscle myoglobin. *Nature* **2001,** 410, (6825), 165-166.

91. Chiti, F.; Dobson, C. M., Amyloid formation by globular proteins under native conditions. *Nat Chem Biol* **2009,** 5, (1), 15-22.

92. Chiti, F.; Taddei, N.; Bucciantini, M.; White, P.; Ramponi, G.; Dobson, C. M., Mutational analysis of the propensity for amyloid formation by a globular protein. *EMBO J* **2000,** 19, (7), 1441-1449.

93. Zandomeneghi, G.; Krebs, M. R. H.; McCammon, M. G.; Fandrich, M., FTIR reveals structural differences between native β-sheet proteins and amyloid fibrils. *Protein Science* **2004,** 13, 3314-3321.

94. Dong, A.; Huang, P.; Caughey, W. S., Protein secondary structures in water from second-derivative amide I infrared spectra. *Biochemistry* **1990,** 29, (13), 3303-3308.

95. Kubelka, J.; Keiderling, T. A., Differentiation of β-Sheet-Forming Structures: Ab Initio-Based Simulations of IR Absorption and Vibrational CD for Model Peptide and Protein β-Sheets. *Journal of the American Chemical Society* **2001,** 123, (48), 12048-12058.

96. Barth, A., The infrared absorption of amino acid side chains. *Progress in Biophysics and Molecular Biology* **2000,** 74, 141-173.

97. Gunzler, H.; Gremlich, H.-U., *IR Spectroscopy*. Wiley-VCH: Weinheim, 2002.

98. Ridgley, D. M.; Claunch, E. C.; Barone, J. R., Characterization of amyloid structures by FT-IR and Raman spectroscopy. *Applied Spectroscopy* **2013,** submitted.

99. Guiffo-Soh, G.; Hernández, B.; Coïc, Y.-M.; Boukhalfa-Heniche, F.-Z.; Ghomi, M., Vibrational Analysis of Amino Acids and Short Peptides in Hydrated Media. II. Role of KLLL Repeats To Induce Helical Conformations in Minimalist LK-Peptides. *The Journal of Physical Chemistry B* **2007,** 111, (43), 12563-12572.

100. Stewart, S.; Fredericks, P. M., Surface-enhanced Raman spectroscopy of amino acids adsorbed on an electrochemically prepared silver surface. *Spectrochimica Acta Part A* **1999,** 55, 1641-1660.

101. Hernandez, B.; Pfluger, F.; Nsangou, M.; Ghomi, M., Vibrational analysis of amino acids and short peptides in hydrated media: IV. Amino acids with hydrophobic

side chains: L-alaine, L-valine, and L-isoleucine. *Journal of Physical Chemistry B* **2009,** 113, 3169-3178.

Chapter 3 Processing and properties of self-assembled polypeptide fiber composites

3.1 Introduction

3.1.1 Composite background

There are many situations, especially in the marine, aerospace, and construction industries, that require a material with unique properties. These properties, such as a combination of high strength and low density, may not exist in just one material. Composites are combinations of two materials that leverage the advantages of each. The most common composite consists of a strong and stiff filler, such as a fiber or particle, embedded at low to moderate volume fraction in a tougher material known as the matrix.[1] The filler is usually more dense than the matrix and the filler appears as discontinuous phases in a continuous matrix. Thus, the filler adds strength and stiffness to the matrix while the matrix provides toughness and low density. Composites exist to optimize combinations of stiffness, strength, density, high-temperature performance, corrosion resistance, hardness, and conductivity.[2] Today composites span a range of uses and exist in both glamorous and not so glamorous roles. Examples of products made from composites are golf clubs, skis, fishing poles, kayaks, tennis rackets, fiberglass boat hulls, automotive tires, and artificial hip and knee joints.[2-4]

The choice of material for the filler and the matrix is determined by the desired combination of properties, intended application, and method of manufacture for the final product. The most common filler is a fiber and these types of composites are known as fiber reinforced composites. Fibers typically have a very high stiffness and a diameter between 10-150 microns.[2] For this reason they are implemented to be the main load

support thus increasing modulus and limiting deformation.[3-5] The fiber also can decrease corrosion, creep, and fatigue.[3] The other component of the composite, the matrix, contributes to the toughness, maintains the desired fiber spacing, transfers loads from the matrix to the fiber, protects the fiber from damage, and prevents cracks in the fiber from propagating throughout the entire composite.[2, 3] A unique characteristic of composites is that their properties can be tailored to fit different types of loading conditions by changing the materials involved or the orientation and type of fibers in the matrix.

A variety of materials can be used for the two components that make up a composite. The first composite was designed by the Egyptians who made bricks out of a mud matrix with straw filler.[2, 4] Today, we have come a long way from mud and straw. In industry, there are three main classes of composite: the most common are polymer matrix composites (PMCs) that usually consist of a polymer matrix embedded with glass, carbon, or aromatic polyamide fibers such as Kevlar.[3-5] Another class is metal matrix composites (MMCs) which are implemented for high temperature use. The third class is ceramic matrix composites (CMCs). CMCs work opposite of PMCs in which the filler contributes to toughness and the matrix provides the majority of the strength.[1, 2] These types of composites are great for a variety of applications because of their ease of manufacture and excellent properties. The main issue with synthetic composites is disposal and PMCs are particularly difficult to recycle because of the close union between the fiber and matrix.[6]

3.1.2 Biobased composites

Wood and bone are examples of fiber PMCs that exist in nature.[1] These have the benefit of being biodegradable and renewable but lack the thermal properties of synthetic plastics.[6] Natural composites do have extraordinary strength, stiffness, and toughness.[7]

There is a current movement that is trying to bridge the gap between the biological and synthetic realms of composite materials by creating biodegradable composites with the desired properties of synthetic composites. In these, one or both components of the composite are biobased and potentially biodegradable. A popular method is to embed biopolymers with natural fibers in which both elements can biodegrade.[6, 8] Biopolymers tend to have low stiffness and strength and a tendency to adsorb moisture, which is why natural fibers and inorganic particles are added to improve mechanical properties and moisture resistance.[9] Biopolymers used in the matrices can be fabricated from renewable resources, synthesized microbially, or synthesized from petroleum based chemicals.[10] Examples of biopolymer matrices include aliphatic polyesters like polylactic acid, thermoplastic starch, soy protein, cellulose acetate, natural rubber, and wheat gluten.[6, 8, 10, 11] Natural fibers are usually plant-based cellulose fibers and act like synthetic glass, carbon, and aramid fibers providing strength and rigidity to the matrix but are usually of lower cost and density and biodegradable.[10, 12, 13] One problem is that natural fibers can vary in properties depending on how they were grown.[6, 14] This problem is not found in synthetic fibers. Biobased composites are an attractive option, but will not be able to be mass-produced until the properties can be controlled better.

Agricultural byproducts, like wheat gluten (WG), are attractive because of their abundance, low cost, good biodegradability, and non-toxicity.[9, 15-17] Wheat gluten in particular has good viscoelastic properties, strong tensile strength, is an excellent gas barrier, and has the ability to fully degrade in less than 50 days making it an ideal byproduct for use in materials.[9, 15, 18, 19] It is found that reinforcement with natural fibers significantly improves the mechanical properties of wheat gluten.[14] There are examples

in the literature of wheat gluten being reinforced with a variety of natural fibers and fillers such as coconut fiber, hydroxyethyl cellulose, jute, nanoclay particles, hemp, and basalt.[9, 13-19] Thus, wheat gluten may be a promising material for biobased composites.

The properties of any composite depend on the size, arrangement, and volume fraction of fiber and on how well the fiber interacts with the matrix.[1, 2] Component compatibility is the most important parameter in the design of any composite because it ensures efficient load transfer from the matrix to the fiber (Figure 3.1). Thus, a lot of engineering goes into achieving a good interface.[1-3] Typical fibers in commodity materials are glass and cellulose and typical matrices are polyolefins. Poor bonding usually occurs because of a hydrophilic fiber in a hydrophobic matrix.[6, 11, 17, 20] The most common way to improve interfacial compatibility is to use a third component, a coupling agent, which has both hydrophilic and hydrophobic chemical groups. Another way is to chemically modify the surface of either the fiber or the matrix.[1, 11] Both of these are often undesirable because of associated added cost, steps, and environmental issues. The only perfect interfaces exist in self-reinforced composites, because the matrix is made of the same material as the composite and therefore they have complete compatibility. These homogenous composites have favor in biomaterials since additives affect biocompatibility and biodegradability and they are generally more recyclable.[21, 22]

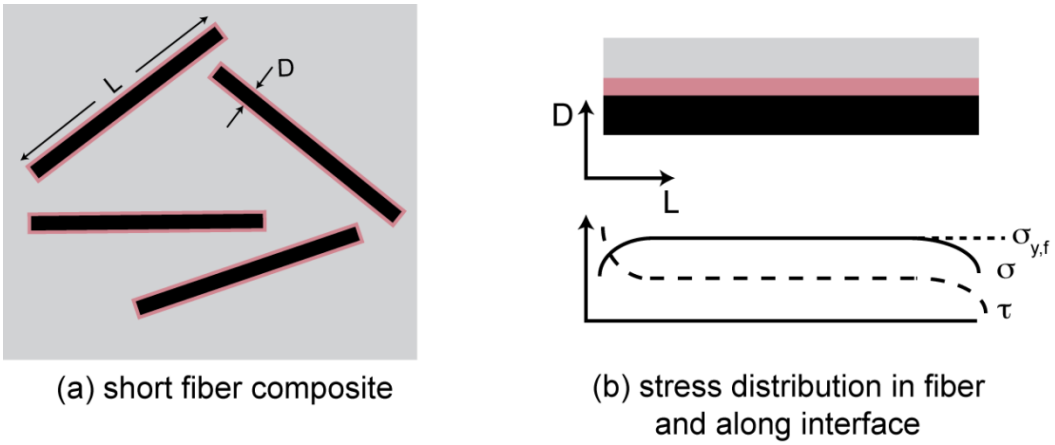

Figure 3.1 (a) Composite morphology showing matrix (gray), fiber (black), and interface (pink) for a fiber composite. (b) Good interfacial interaction between the polymer matrix and the reinforcing fiber is needed to achieve good stress transfer from the matrix to the fiber when the composite is stressed, σ.

Another problematic area for biobased composites is processing. Composites are manufactured by a variety of techniques including compression molding, injection molding, resin transfer molding, hand lay-up or spray up, winding, pultrusion, and extrusion or melt compounding.[4, 5] The forming process can position the fibers in a desired orientation so that they can be oriented relevant to the loading direction in the product or the fibers can simply be randomly oriented.[5] In oriented fiber geometries, the properties are always highest along the fiber direction.[1, 2, 4] A problem with the manufacture of biobased composites is the low processing temperature required to prevent degradation during processing.[6] For this reason, the thermal processing used in synthetic composite manufacture may not be suitable for biobased composites.[12, 14] WG has been processed using extrusion, compression molding, and solution casting but events during processing can decrease mechanical properties.[13, 14, 19] This is not favorable, especially when biobased composites are trying be competitive with synthetic composites.

One way to avoid degradation during processing may be to fabricate composites by self-assembly. Self-assembly is the spontaneous association of molecules or nanoparticles into larger scale structures and is a process found in many naturally occurring materials.[23] One composite processing method that utilizes self-assembly is layer by layer fabrication.[24-27] This process has gained popularity because the production is simple, there is systematic control over the structure and the thickness of the films, and there is versatility in the application and materials that can be used.[23, 24] Materials that have been shown to self-assemble into films are small organic molecules, inorganic compounds, macromolecules, biomacromolecules (proteins), DNA, and colloids.[24] Hydrogen bonding is the common driving force for layer by layer fabrication of thin films. Core-corona polymers were synthesized and self-assembled by hydrogen bonding to form raspberry-shaped composites.[25] Dendrimer-coated gold nanoparticles self-assembled into composite films with conductive properties.[27] Self-assembled composites are especially desirable for medical and semiconductor applications because you can tune the materials properties at the molecular level.[27] In the medical field, self-assembled systems are being developed for drug delivery[25, 28] and tissue engineering scaffolds.[29, 30]

While wheat gluten is a promising material for biobased composites, poor fiber/matrix bonding and processing degradation have been observed. The poor bonding could be solved by self-reinforcing the wheat gluten. Similarly, processing degradation can be avoided by making the composite through self-assembly. We have shown that trypsin-hydrolyzed wheat gluten will produce a series of polypeptides where some of the polypeptides will self-assemble into very high rigidity fibers and the rest will not, thus remaining as the continuous matrix.[31-34] Self-assembled wheat gluten fiber composites

are processed in aqueous solution at neutral pH by allowing the fibers to form in a matrix of unassembled polypeptides. The fiber and the matrix phases are produced from the same polypeptide solution and the potential exists for good fiber/matrix adhesion. In this study, self-assembled wheat gluten composites are formed and then characterized with 3-point bend (3PB) mechanical testing, scanning electron microscopy (SEM), and Fourier transform infrared (FTIR) spectroscopy.

3.2 Materials and Methods

3.2.1 Hydrolyzed wheat gluten.

4 g of Wheat Gluten (MP Biomedicals, LLC, Solon, OH) were dissolved in 160 ml of pure water and hydrolyzed with 60 mg of trypsin (Type I from bovine pancreas, Sigma-Aldrich, St. Louis, MO) at a 1:67 enzyme to substrate ratio (w/w). The solution was maintained at pH 8 with 1 M NaCl, 37^{o}C, and constant stirring for 120 days. This procedure has been shown to be a high fiber producer.[33] Another high fiber producing composite was prepared in the same manner but was maintained at pH 4 instead of pH 8. A control was prepared by allowing hydrolysis for 1 day at 37^{o}C then decreasing the temperature to room temperature for 120 days. Room temperature inhibited fiber formation so this procedure produced a fiberless material.[33]

3.2.2 Formation of composite.

After 1 day of hydrolysis, the solutions were pipetted into silicone molds with a 12.5 mm diameter, 2.75 mm height, and 33.7 cm^3 volume. The polypeptide concentration in solution was 25 mg/ml so the mold filled with solution did not contain much polypeptide. The molds were allowed to dry under a fume hood. When the solution dried it created more room allowing for new solution to be pipetted into the mold each day. This process

continued until the mold was filled with solid material. The filled mold was then allowed to completely dry in a 37^{o}C chamber for 10 days to remove excess water.

3.2.3 Mechanical properties.

3 point bending (3PB) was performed using a modified version of ASTM D790, which is the standard that has been used for other wheat gluten composites.[12, 17, 18, 20] 3-point bending was performed on a Com-Ten Industries 95 RC Test System with a load cell of 100 kg. A span width of 7 mm and a crosshead speed 1 mm/min was used.

3.2.4 Fourier Transform Infrared (FTIR) Spectroscopy.

Composites were dried overnight under vacuum to remove any excess water. Attenuated total reflectance (ATR) FTIR spectra of the composites were recorded on a Thermo Nicolet 6700 FTIR Spectrometer (Thermo Fisher Scientific Inc., Madison, WI). Samples were loaded into a Smart Orbit ATR Diamond Crystal and spectra were acquired at 256 scans at 4 cm^{-1} resolution from 4000-525 cm^{-1} with a blank background.

3.2.5 Scanning electron microscope (SEM).

Fractured 3PB samples were dried overnight under vacuum to remove excess water. Fractured specimens, with the fracture surface pointing up, were mounted onto aluminum SEM stubs with double-sided tape. Scanning electron micrographs of the fracture surface were obtained using a LEO 1550 field-emission SEM (Zeiss, Peabody, MA) with a 4-6 mm working distance, 5 kV accelerating voltage, and an In-lens SE-detector. Fiber dimensions, volume fracture and interfacial interactions were observed from these images.

3.3 Results and Discussion

3.3.1 Self – assembled WG composites

WG composites are formed from peptide mixtures that contain a template and an adder, a process demonstrated in Figure 3.2. The template and adder work together to form a fiber and the non-assembling peptide left in solution make up matrix. SEM imaging of the fracture surface after 3PB confirmed the fabrication of fiber reinforced composites through self-assembly process (Figure 3.3). The composites have an average diameter of 12.2 ± 0.04 mm and a height of 2.6 ± 0.08 mm. Figure 3.3 a shows 5 fibers embedded in the matrix over a surface area of roughly 250 mm^2. The fibers observed are about 10 microns in diameter. The WG composite is slightly different from those manufactured by highly controlled processes. Instead of the fibers being oriented in one direction, the self-assembly process lends itself toward a random distribution of the fibers in the matrix (Figure 3.3 b). This results in a composite that resembles more of a short fiber random oriented composite.

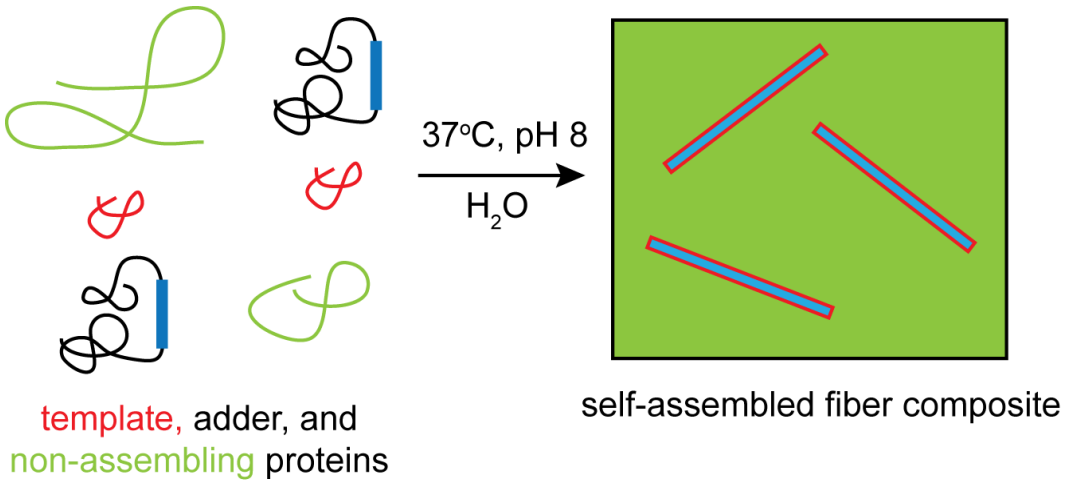

Figure 3.2 The process by which a WG composite is self-assembled

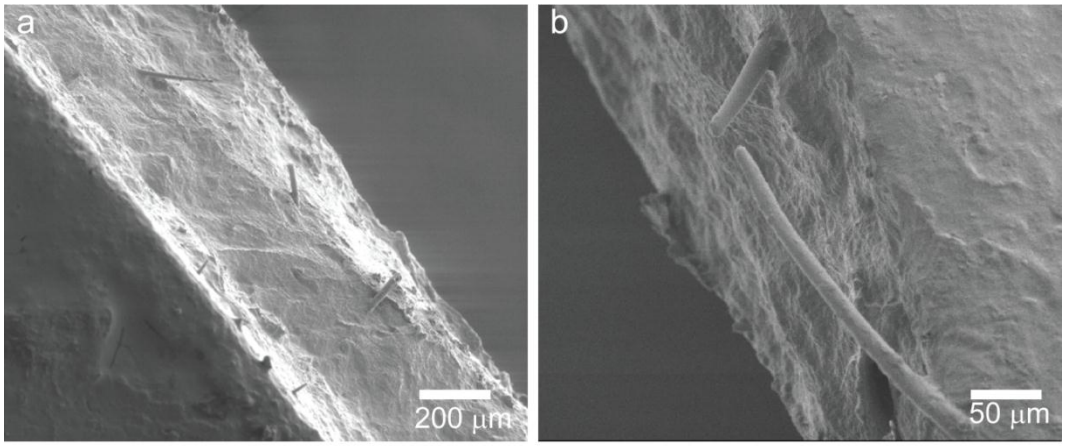

Figure 3.3 SEM images taken from the top looking over the edge of WG composites after 3PB highlight (a) self-assembled fiber formation and (b) random orientation of fibers within the matrix. WG fibers are approximately 10 μm in diameter.

As predicted, the WG composites appear to have good interfacial interaction between the fiber and the matrix. Fiber pull out does not seem to be an issue as observed with previous WG reinforced composites.[17, 20] Instead, an observation is that the matrix was pulled with the fiber during fracture, which is an indicator of good bonding between the two. Figure 3.4a shows that the fiber failed by tearing. There are also no gaps between the broken fibers and the matrix, an indication of good adherence (Figure 3.4a and b). This method of manufacture is ideal with respect to interfacial interaction because both components of the composite are contrived from the same WG solution. Thus, there is near perfect compatibility between the fiber and matrix, so there is no need for a coupling agent or for surface modification.

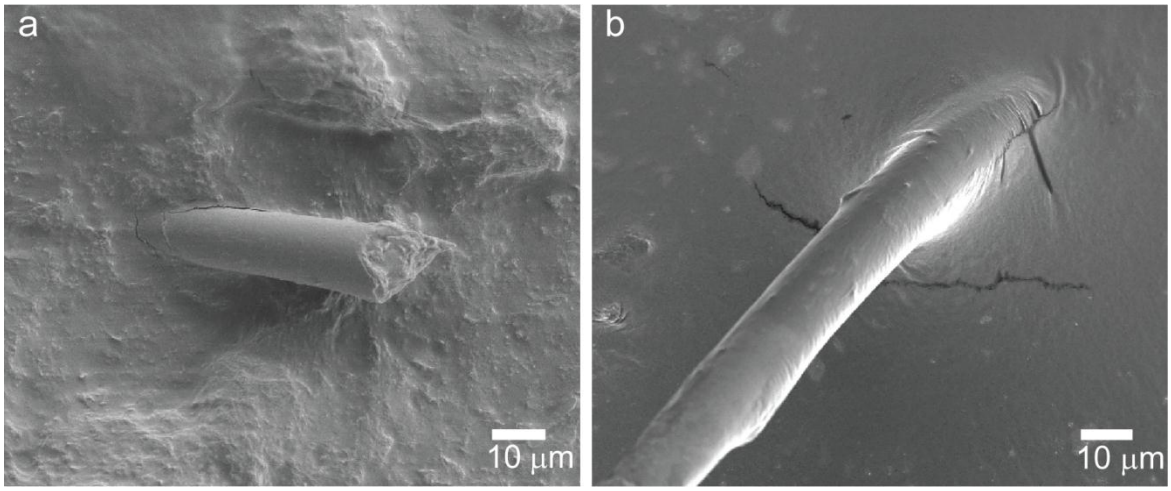

Figure 3.4 SEM images of fibers observed in (a) fiber forming conditions and (b) fiber formed under suppressed fiber forming conditions highlight the good adhesion between the fiber and matrix.

3.3.2 Mechanical properties.

In previous work we have shown that you can change amyloid content of a solution by changing the processing conditions. Composites with these conditions were made because changing amyloid content has the ability to change mechanical properties of the composite. 3 point bending was performed to measure the tensile strength of the WG composite. A representation of the 3PB data for the fiber forming composites (WG pH 8 at 37^{o}C and WG pH 4 at 37^{o}C) and the control (WG pH 8 at room temperature) along with corresponding SEM images of the composite are shown in Figure 3.5 a-c. From this data, the Young's Modulus was determined from the slope of the elastic portion of the stress-strain curve. The strain to fracture was determined as strain at point of first fracture; these values can be found in Table 3.1. For pH 8 at 37^{o}C, the Young's modulus varies from 0.45 to 5.23 MPa with an average of 2.41 MPa and an average strain to fracture of 0.05. These values can be split into two groups; a lower modulus group with an average Young's modulus of 0.81 MPa and the higher modulus group having an average of 4.0 MPa.

Table 3.1 Results of 3PB for the fiber forming composites and composites under suppressed fiber formation.

Composite	Modulus (MPa)	Strain to Fracture
pH 8 RT	2.40	0.13
	1.79	0.20
	1.75	0.08
	1.47	0.19
Average	1.85	0.15
pH 8 37 °C	5.23	0.04
	4.42	0.03
	3.40	0.04
	2.93	0.04
Average high modulus	4.00	0.04
	1.21	0.05
	0.89	0.04
	0.71	0.03
	0.45	0.10
Average low modulus	0.82	0.06
Average	2.41	0.05
pH 4 37 °C	19.10	0.02
	12.69	0.04
	59.37	0.02
	41.18	0.04
Average	33.09	0.03

The highest modulus was observed for the pH 4 composites, having an average of 33.09 MPa. This composite also had the smallest strain to fracture and a stress-strain graph resembling brittle failure (Figure 3.5c). This composite, like the pH 8 at 37^{o}C showed large variation with Young's modulus ranging from 12.69 to 59.37 MPa. The control composite, however, showed less variation, the average modulus is 1.85 MPa and the average strain to fracture is 0.15. The SEM images of the control showed similar results to that of the lower modulus fiber forming group in which fiber production was either reduced or eliminated. These observations lead to the conclusion that fibers

influence the mechanical properties of the composite. It is a known occurrence that increasing the number of fibers within a composite will increase the mechanical properties.[11]

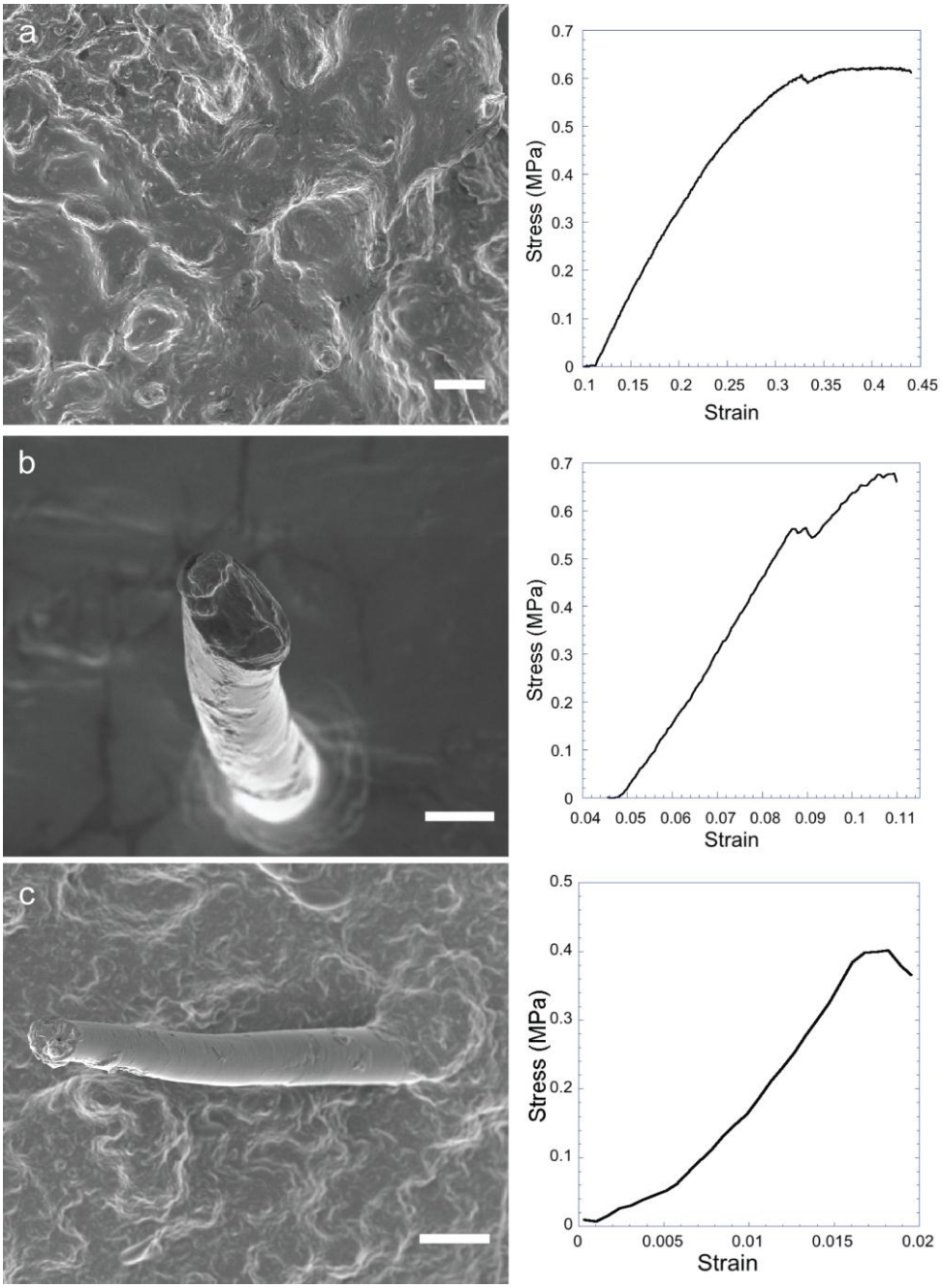

Figure 3.5 SEM images paired with stress-strain plots for WG composites (a) pH 8 RT , (b) WG pH 8 37° C (c) WG pH 4 37° C. Scale bar represents 10 μm.

After comparing the SEM images with the 3PB results (figure 3.5 a-c) for each group of composites it can be concluded that the variations in this data are related to the number of fibers present in the composite and to an uneven distribution of the fibers. The composites with lower moduli have either fewer fibers or no fibers visible in SEM compared with the composites that have higher moduli. The fact that there are no fibers in the control contributes to the why it showed the smallest variation in Young's Modulus of the three systems. It has been observed with WG and hemp fiber composites that increasing the percentage of fibers from 5% to 20% increased the Young's modulus of the material from 15.80 ± 4.0 to 81.32 ± 14.2 MPa and decreased fracture strain from 10.70 ± 10.5 to 2.63 ± 2.5 [13] in one case, and increased Young's Modulus from 41.4 ± 14.3 to 227.1 ± 93.5 MPa and decreased fracture strain of 45.9 ± 17.4 to 8.6 ± 2.2[14] in another case. Although the values of elastic modulus are much higher than observed in our WG composites, the trend of increasing fiber percentage to increase modulus holds true and that Young's modulus positively correlates and fracture strain negatively correlates with the percentage of fibers.[14]

The Young's modulus for previous reinforced WG composites is higher than what is observed in the self-assembled composites. A modulus of 65 MPa was observed with 30% hydroxethyl cellulose filler[9], the optimized modulus of elasticity for WG with 40% jute fiber composites was found to be very high at 2928 ± 259 MPa[16], and similarly WG with 15% unmodified coconut fiber filler was found to have a modulus of 2.8 ± 0.2 GPa.[17] These values are much higher than that of the self-assembled WG composites which is impart do to the volume fraction. For the self-assembled WG fiber forming composites, the volume fraction is not controlled and is most likely lower than the

percentages reported for the reinforced WG composites. A higher percentage of fibers results in higher mechanical properties. The hydroxethyl cellulose, jute fibers, and coconut fibers probably also have a higher stiffness than the WG fibers that are embedded in our composite, another factor that would contribute to a higher modulus.

FT-IR was performed on the solid state composites to determine if the fibers within the composite were of amyloid nature. β-sheet content was determined as the Amide I peak divided by Amide II. The composites with higher levels of fiber formation also had higher elastic moduli (Figure 3.6). This implies that amyloid fibers, associated with dense regions of β-sheets, play a role in providing strength to the composite. A major concept in materials science is that molecular structure determines morphology and properties. High density of β-sheet provides a unique, robust structure for the fiber, thus providing reinforcement to the composite. Thus, amyloids can be a useful structurally in forming bio-based composites.

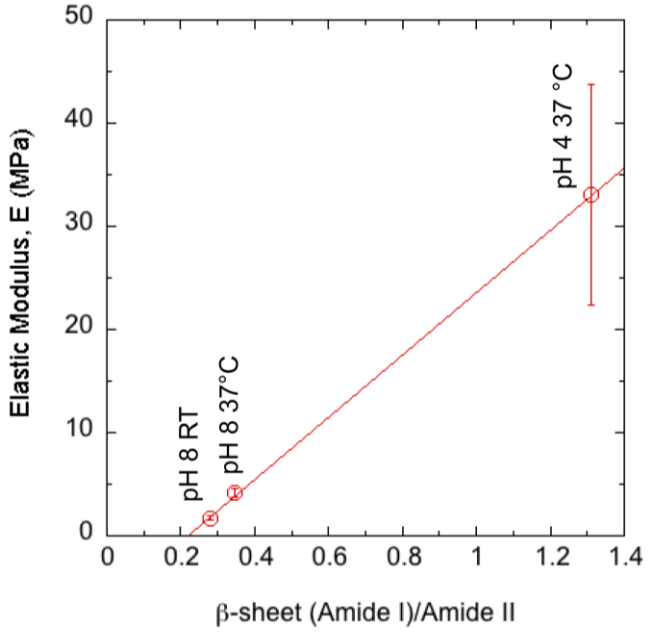

Figure 3.6 Elastic modulus (Young's modulus) positively correlates with β-sheet content. This points toward the conclusion that amyloid fibers provide strength to the composite.

3.4 Conclusion

WG composites were successfully self-assembled from a mixture of polypeptides where 2 polypeptides cooperatively form the fiber and a 3rd does not self-assemble and forms the matrix. The processing and mechanical behavior of these self-reinforced fiber composites were studied. Processing conditions can be used to affect β-sheet formation, protein interactions, and fiber production to vary modulus. There was variation within the WG composites that was related to the distribution of fibers both within each composite and between the composite groups. It was concluded that Young's modulus positively correlates and fracture strain negatively correlates with the percentage of fiber in the composite. Although the mechanical properties are not yet competitive with previous reinforced WG composites, there are other benefits associated with the homogeneity of the matrix and fiber such as near perfect interfacial interaction that is obtained without additives.

The self-assembly process offers a low cost, low energy option for manufacturing of composites. Self-assembly avoids the processing degradation of WG that has been observed with thermal processing. Although it is still not competitive with commercial polymer composites in terms of mechanical performance or ease of bulk manufacture, WG is a promising biomaterial for use in composites. This paper focused on advancing the uses of WG as a biomaterial by improving the poor bonding and mechanical degradation observed in previous WG composites.

Acknowledgements

Generous funding through NSF-CMMI-0856262 and the Virginia Tech Biodesign and Bioprocessing Research Center are greatly appreciated.

References

1. Hull, D.; Clyne, T. W., *An introduction to composite materials*. 2nd ed.; Cambridge University Press: Cambridge ; New York, 1996; p xvi, 326 p.

2. Askeland, D. R., *The science and engineering of materials*. 3rd ed.; PWS Pub.: Boston, 1994; p xx, 812 p.

3. Sperling, L. H., *Introduction to physical polymer science*. 4th ed.; Wiley: Hoboken, N.J., 2006; p xxx, 845 p.

4. Fried, J. R., *Polymer science and technology*. 2nd ed.; Prentice Hall Professional Technical Reference: Upper Saddle River, NJ, 2003; p xvii, 582 p.

5. McCrum, N. G.; Buckley, C. P.; Bucknall, C. B., *Principles of polymer engineering*. 2nd ed.; Oxford University Press: Oxford ; New York, 1997; p xiv, 447 p.

6. Mohanty, A. K.; Misra, M.; Hinrichsen, G., Biofibres, biodegradable polymers and biocomposites: An overview. *Macromolecular Materials and Engineering* **2000,** 276-277, (1), 1-24.

7. Vincent, J., *Structural Biomaterials*. Princeton University Press: Princeton, 1990.

8. Averous, L.; Boquillon, N., Biocomposites based on plasticized starch: thermal and mechanical behaviours. *Carbohydrate Polymers* **2004,** 56, (2), 111-122.

9. Song, Y.; Zheng, Q.; Liu, C., Green biocomposites from wheat gluten and hydroxyethyl cellulose: Processing and properties. *Industrial Crops and Products* **2008,** 28, (1), 56-62.

10. Mohanty, A. K.; Misra, M.; Drzal, L. T., Sustainable Bio-Composites from Renewable Resources: Opportunities and Challenges in the Green Materials World. *Journal of Polymers and the Environment* **2002,** 10, (1-2), 19-26.

11. Bhowmick, M.; Mukhopadhyay, S.; Alagirusamy, R., Mechanical properties of natural fibre-reinforced composites. *Textile Progress* **2012,** 44, (2), 85-140.

12. Mohanty, A. K.; Wibowo, A.; Misra, M.; Drzal, L. T., Effect of process engineering on the performance of natural fiber reinforced cellulose acetate biocomposites. *Composites Part A: Applied Science and Manufacturing* **2004,** 35, (3), 363-370.

13. Kunanopparat, T.; Menut, P.; Morel, M. H.; Guilbert, S., Reinforcement of plasticized wheat gluten with natural fibers: From mechanical improvement to deplasticizing effect. *Composites Part A: Applied Science and Manufacturing* **2008,** 39, (5), 777-785.

14. Wretfors, C.; Cho, S. W.; Hedenqvist, M. S.; Marttila, S.; Nimmermark, S.; Johansson, E., Use of Industrial Hemp Fibers to Reinforce Wheat Gluten Plastics. *Journal of Polymers and the Environment* **2009,** 17, (4), 259-266.

15. Zhang, X.; Do, M. D.; Dean, K.; Hoobin, P.; Burgar, I. M., Wheat-Gluten-Based Natural Polymer Nanoparticle Composites. *Biomacromolecules* **2007,** 8, (2), 345-353.

16. Reddy, N.; Yang, Y., Biocomposites developed using water-plasticized wheat gluten as matrix and jute fibers as reinforcement. *Polymer International* **2011,** 60, (4), 711-716.

17. Hemsri, S.; Grieco, K.; Asandei, A. D.; Parnas, R. S., Wheat gluten composites reinforced with coconut fiber. *Composites Part A: Applied Science and Manufacturing* **2012,** 43, (7), 1160-1168.

18. Ye, P.; Reitz, L.; Horan, C.; Parnas, R., Manufacture and Biodegradation of Wheat Gluten/Basalt Composite Material. *Journal of Polymers and the Environment* **2006,** 14, (1), 1-7.

19. Kunanopparat, T.; Menut, P.; Morel, M.-H.; Guilbert, S., Plasticized wheat gluten reinforcement with natural fibers: Effect of thermal treatment on the fiber/matrix adhesion. *Composites Part A: Applied Science and Manufacturing* **2008,** 39, (12), 1787-1792.

20. Herrera-Franco, P. J.; Valadez-González, A., Mechanical properties of continuous natural fibre-reinforced polymer composites. *Composites Part A: Applied Science and Manufacturing* **2004,** 35, (3), 339-345.

21. Gao, C.; Yu, L.; Liu, H.; Chen, L., Development of self-reinforced polymer composites. *Progress in Polymer Science* **2012,** 37, (6), 767-780.

22. Matabola, K. P.; Vries, A. R.; Moolman, F. S.; Luyt, A. S., Single polymer composites: a review. *Journal of Materials Science* **2009,** 44, (23), 6213-6222.

23. Fendler, J. H., Self-Assembled Nanostructured Materials. *Chemistry of Materials* **1996,** 8, (8), 1616-1624.

24. Zhang, H.; Wang, Z.; Zhang, Y.; Zhang, X., Hydrogen-Bonding-Directed Layer-by-Layer Assembly of Poly(4-vinylpyridine) and Poly(4-vinylphenol): Effect of Solvent Composition on Multilayer Buildup. *Langmuir* **2004,** 20, (21), 9366-9370.

25. Li, R.; Yang, X.; Li, G.; Li, S.; Huang, W., Core−Corona Polymer Composite Particles by Self-Assembled Heterocoagulation Based on a Hydrogen-Bonding Interaction. *Langmuir* **2006,** 22, (19), 8127-8133.

26. Kotov, N. A.; Dekany, I.; Fendler, J. H., Layer-by-Layer Self-Assembly of Polyelectrolyte-Semiconductor Nanoparticle Composite Films. *The Journal of Physical Chemistry* **1995,** 99, (35), 13065-13069.

27. Krasteva, N.; Besnard, I.; Guse, B.; Bauer, R. E.; Müllen, K.; Yasuda, A.; Vossmeyer, T., Self-Assembled Gold Nanoparticle/Dendrimer Composite Films for Vapor Sensing Applications. *Nano Letters* **2002,** 2, (5), 551-555.

28. He, X.; Ge, X. W.; Wang, M.; Zhang, Z., Polystyrene/melamine-formaldehyde hollow microsphere composite by self-assembling of latex particles at emulsion droplet interface. *Polymer* **2005,** 46, (18), 7598-7604.

29. Horii, A.; Wang, X.; Gelain, F.; Zhang, S., Biological Designer Self-Assembling Peptide Nanofiber Scaffolds Significantly Enhance Osteoblast Proliferation, Differentiation and 3-D Migration. *PLoS ONE* **2007,** 2, (2), e190.

30. Tampieri, A.; Celotti, G.; Landi, E.; Sandri, M.; Roveri, N.; Falini, G., Biologically inspired synthesis of bone-like composite: Self-assembled collagen fibers/hydroxyapatite nanocrystals. *Journal of Biomedical Materials Research Part A* **2003,** 67A, (2), 618-625.

31. Athamneh, A.; Barone, J. R., Enzyme-mediated self-assembly of highly ordered structures from disordered proteins. *Smart Materials and Structures* **2009,** 18, 104024 (8pp).

32. Ridgley, D. M.; Ebanks, K. C.; Barone, J. R., Peptide mixtures can self-assemble into large amyloid fibers of varying size and morphology. *Biomacromolecules* **2011,** 12, (10), 3770-3779.

33. Ridgley, D. M.; Claunch, E. C.; Barone, J. R., The effect of processing on large, self-assembled amyloid fibers. *Soft Matter* **2012,** 8, (40), 10298-10306.

34. Ridgley, D. M.; Barone, J. R., Evolution of the amyloid fiber over multiple length scales. *ACS Nano* **2013,** 7, (2), 1006-1015.

35. Miyazawa, T.; Shimanouchi, T.; Mizushima, S.-i., Characteristic Infrared Bands of Monosubstituted Amides. *The Journal of Chemical Physics* **1956,** 24, (2), 408-418.

36. Surewicz, W. K.; Mantsch, H. H., New insight into protein secondary structure from resolution-enhanced infrared spectra. *Biochimica et Biophysica Acta* **1988,** 952, 115-130.

37. Blout, E. R.; Idelson, M., Polypeptides. VI. Poly-α-L-glutamic acid: Preparation and helix-coil conversion. *Journal of the American Chemical Society* **1956,** 78, 497-498.

38. Lenormant, H.; Baudras, A.; Blout, E. R., Reversible configurational changes in sodium poly-α-L-glutamate induced by water. *Journal of the American Chemical Society* **1958,** 80, 6191-6195.

39. Fraser, R. D. B.; Harrap, B. S.; MacRae, T. P.; Stewart, F. H. C.; Suzuki, E., Effect of glycyl residues on the stability of the α-helix. *Biopolymers* **1967,** 5, 221-257.

40. Nevskaya, N. A.; Chirgadze, Y. N., Infrared spectra and resonance interactions of amide-I and II vibrations of α-helix. *Biopolymers* **1976,** 15, (4), 637-648.

41. Vendantham, G.; Sparks, H. G.; Sane, S. U.; Tzannis, S.; Przybycien, T. M., A holistic approach for protein secondary structure estimation from infrared spectra in H_2O solutions. *Analytical Biochemistry* **2000,** 285, 33-49.

42. Goormaghtigh, E.; Cabiaux, V.; Ruysschaert, J.-M., Secondary structure and dosage of soluble and membrane proteins by attenuated total reflection Fourier-transform

infrared spectroscopy on hydrated films. *European Journal of Biochemistry* **1990,** 193, (2), 409-420.

43. Fraser, R. D. B.; MacRae, T. P., *Conformation in Fibrous Proteins and Related Synthetic Polypeptides*. Academic Press: New York, 1973.

44. Kumosinski, T. F.; Unruh, J. J., Quantitation of the global secondary structure of globular proteins by FTIR spectroscopy: Comparison with X-ray crystallographic structure. *Talanta* **1996,** 43, (2), 199-219.

45. Balbirnie, M.; Grothe, R.; Eisenberg, D. S., An amyloid-forming peptide from the yeast prion Sup35 reveals a dehydrated β-sheet structure for amyloid. *Proceedings of the National Academy of Sciences* **2001,** 98, (5), 2375-2380.

46. Vecchio, G.; Bossi, A.; Pasta, P.; Carrea, G., Fourier-transform infrared conformational study of bovine insulin in surfactant solutions. *International Journal of Peptide and Protein Research* **1996,** 48, (2), 113-117.

47. Halverson, K.; Fraser, P. E.; Kirschner, D. A.; Lansbury, P. T., Molecular determinants of amyloid deposition in Alzheimer's disease: conformational studies of synthetic β-protein fragments. *Biochemistry* **1990,** 29, (11), 2639-2644.

48. Bouchard, M.; Zurdo, J.; Nettleton, E. J.; Dobson, C. M.; Robinson, C. V., Formation of insulin amyloid fibrils followed by FTIR simultaneously with CD and electron microscopy. *Protein Science* **2000,** 9, (10), 1960-1967.

49. Krimm, S.; Bandekar, J., Vibrational spectroscopy and conformation of peptides, polypeptides, and proteins. In *Advances in Protein Chemistry*, Anfinsen, C. B.; Edsall, J. T.; Richards, F. M., Eds. Academic Press, Inc.: Orlando, 1986; Vol. 38, pp 181-364.

50. Fandrich, M.; Fletcher, M. A.; Dobson, C. M., Amyloid fibrils from muscle myoglobin. *Nature* **2001,** 410, (6825), 165-166.

51. Chiti, F.; Dobson, C. M., Amyloid formation by globular proteins under native conditions. *Nat Chem Biol* **2009,** 5, (1), 15-22.

52. Chiti, F.; Taddei, N.; Bucciantini, M.; White, P.; Ramponi, G.; Dobson, C. M., Mutational analysis of the propensity for amyloid formation by a globular protein. *EMBO J* **2000,** 19, (7), 1441-1449.

53. Fandrich, M.; Forge, V.; Buder, K.; Kittler, M.; Dobson, C. M.; Diekmann, S., Myoglobin forms amyloid fibrils by association of unfolded polypeptide segments. *Proceedings of the National Academy of Sciences* **2003,** 100, (26), 15463-15468.

Chapter 4 Conclusion

4.1 Summary of work

The benefits of amyloids to the materials world have been discussed and two applications have been studied. Although time and availability did not allow the use of many characterization techniques, a sufficient amount was done to determine the presence of amyloid fibers. Two of the three characteristics of amyloid fibers were confirmed. For all systems observed, fibrillar structure was confirmed with either SEM or AFM. The content of β- sheet secondary structure was observed with FT-IR on both aqueous solution and in dried form for the morphology studies and for the composite.

It was shown that the morphology of a peptide solution can be controlled by altering the concentration of the solution in which lower concentrations predominately formed fibrils and higher concentrations predominately formed globules. Fibril formation did not necessarily depend on β-sheet content, because fibrils had lower β-sheet content than globules. Amide glutamine hydrogen bonding was also not a necessity for fibril formation, but it did aid in the formation process. Fibrils did however require interdigitation of CH_3 groups on A, I, L, and V that occur concurrently with glutamine amide hydrogen bonding. Globules did not require this and formed from more random hydrophobic interactions that preceded glutamine amide hydrogen bonding.

It was also shown that Fiber composites can be self-assembled from a mixture of polypeptides where 2 polypeptides cooperatively form the fiber and a 3rd does not self-assemble and forms the matrix. Since the polypeptides in solution are similar, there is good fiber/polymer chemical interaction. It was also observed that processing conditions

such as pH and temperature can be used to affect β-sheet formation, protein interactions, and fiber production to vary modulus of the composite.

4.2 Future work

Since morphology plays a role in mechanical strength, future work would include testing the mechanical properties of both the fibril and globule. Another area of future study would be to create a self-assembled amyloid coating similar to barnacle adhesive that could act as an antifouling coating. This self-assembled protein coating would be at equilibrium and would potentially discourage barnacle proteins introduced by the organism to further self-assemble and attach to the surface. Biofouling is a huge problem, so it would be a great achievement if a non-toxic functional coating could be engineered.

The main area of improvement for the composite system is through control of the modulus. An increased modulus value would be necessary for the composite to be competitive in industry. This could be achieved by optimizing the processing conditions to increase the volume fraction of the fibers in the composite. Controlling the amount and even orientation of the fibers would not only reduce variation between composite moduli, but would also aid in increasing the modulus to something that could be of use.

4.3 Conclusions

These systems offer insight into different applications for amyloids in relation to materials. One area is the control of material properties through the regulation of the morphology. Being able to control a material's properties in this manner could lead to nanoscale control over processing and/or development from the bottom up of submicron scale materials. These types of materials would be key components for advances in biomedical and technological fields.

The second area of application is as the filler, offering structural support for a biological composite. Composites are ubiquitous in everyday life. A composite composed entirely of a biological material such as WG would be environmentally favorable. Also, the self-assembly process under which it is formed offers a low energy, low cost process for the manufacture of these composites. Areas where biological protein composites may have a future are in the development of lightweight materials for application in cars, airplanes, and buildings which would reduce energy consumption and the ecological footprint of the materials.

Understanding the relationship between biology, engineering, and material science may open doors for future materials. Nature's design process is complex but results in materials with unique properties yet to be achieved by synthetic design. The key is to unlock the secrets to these processes and apply them in useful ways. Function amyloids may be one area where this can be achieved. The fibers can be formed by a wide range of proteins and be tailored to a variety of applications. Highlighted in this research were only a few of the many applications for which functional amyloids show promise.